

## The High-Resolution Rotational and Torsional Spectra of HSSH

STEPAN URBAN,<sup>1</sup> ERIC HERBST,<sup>2</sup> PETRA MITTLER, GISBERT WINNEWISSER,  
AND KOICHI M. T. YAMADA*I. Physikalisches Institut, Universität zu Köln, D-5000 Köln 41, Federal Republic of Germany*

AND

MANFRED WINNEWISSER

*Physikalisch-Chemisches Institut, Justus-Liebig Universität, D-6300 Giessen,  
Federal Republic of Germany*

High-resolution spectroscopic measurements on both the torsional and the rotational spectra of disulfane (HSSH) are reported. The infrared torsional spectrum has been measured using a high-resolution Fourier transform spectrometer in the range 300–550  $\text{cm}^{-1}$ . Approximately 2000 torsional-rotational spectral lines belonging to the band systems  $v_t = 1 \leftarrow 0$ ,  $2 \leftarrow 1$ , and  $3 \leftarrow 2$  have been analyzed and fitted. In addition, new rotational transitions are reported, especially involving the second excited ( $v_t = 2$ ) torsional state. The torsional potential function of Herbst and Winnewisser (*Chem. Phys. Lett.* 155, 572–575 (1989)) has been refined. © 1989 Academic Press, Inc.

## I. INTRODUCTION

Disulfane (HSSH), a nearly accidental prolate symmetric top, exhibits a number of interesting spectroscopic effects that can be measured, disentangled, and studied to a high level of clarity. The nearly right-angle chain structure and the high barrier toward internal rotation are in the main responsible for these effects, which are detected by high-resolution spectroscopy.

First and foremost, HSSH and all of its presently known isotopically substituted forms are nearly perfect accidental prolate symmetric tops with asymmetry parameter  $\kappa$  varying between  $-0.9996$  for HSSH and  $-0.9999993$  for DSSD (1–3). The  $r_0$  structure of the molecule is such that the dihedral angle  $\chi$  is only slightly greater than  $90^\circ$  (the *gauche* configuration) with potential barriers at both the *trans* ( $\chi = 180^\circ$ ) and *cis* ( $\chi = 0^\circ$ ) configurations. In addition, the HSS bond angle is approximately  $99^\circ$ , so that this angle is nearly perpendicular as well. The dipole moment of HSSH lies perpendicular to the S–S axis, which results in *c*-type transitions if the dihedral angle exceeds about  $90^\circ$  (1). The rotational and rovibrational spectra consist of regularly

<sup>1</sup> Permanent address: J. Heyrovsky Institute of Physical Chemistry and Electrochemistry, Czechoslovak Academy of Sciences, Praha, Dolejskova ul. 3, 182 23 Prague 8, CSSR.

<sup>2</sup> Alexander von Humboldt Awardee. Permanent address: Department of Physics, Duke University, Durham, North Carolina 27706.

spaced compact  $Q$ -branches and easily discernable  $P$ - and  $R$ -branches. The  $K$ -type doubling in molecules with small asymmetry is caused by two effects: splitting due to the  $\Delta K = \pm 2$  asymmetric top matrix elements ("asymmetry splitting") and centrifugal distortion splitting due to the matrix elements of the quartic, sextic, and higher-order distortion terms. The  $K$ -type doubling induced by centrifugal distortion was first observed in the millimeter-wave spectra of HSSH and DSSD (2, 3).

Second, significant differences occur between the various isotopic species that are symmetric to exchange (e.g., HSSH, DSSD) and those that are not (e.g., HS<sup>34</sup>SH, HSSD). The symmetric isotopes show an alternation in intensity due to nuclear spin statistics which is missing in the nonsymmetric isotopes. These latter isotopes can exhibit both  $b$ - and  $c$ -type transitions due to a rotation of the principal axes. This effect is most marked for HSSD (2) and DS<sup>34</sup>SD (manuscript in preparation).

Third, the torsional splittings in disulfane are fairly small and not very dependent on rotational quantum numbers. They can therefore be used to test theoretical aspects of internal motion and to obtain the potential energy for torsional motion to a high degree of accuracy. The effects of differing *cis* and *trans* barriers can be seen in the spectra, although they are not as dominant as in HOOH, due to the higher barriers in HSSH. Although torsional motion is almost always treated as an effective one-dimensional motion, the relative simplicity of the HSSH torsional spectrum caused by the high barriers to internal rotation and the small number of normal modes allows a determination of the coupling of the torsional motion to other modes of motion, in particular the low-frequency S-S stretch.

Finally, the structure of HSSH as well as its torsional barriers are an excellent testing ground for ab initio quantum chemical treatments. Indeed, presently available torsional barriers and equilibrium structures from a variety of ab initio calculations are in excellent agreement with the experimentally determined  $r_0$  structure and torsional potential, as shall be discussed later.

These interesting features have made disulfane a topic for a significant amount of spectroscopic investigation. A large body of data in both the millimeter-wave and infrared regions of the spectrum as well as Raman and electron diffraction work has been published (1-11). Recently, Herbst and Winnewisser (11) have derived a potential function for the torsional motion of HSSH based on a limited amount of experimental data, including torsional splittings in the ground ( $v_t = 0$ ) and first excited ( $v_t = 1$ ) torsional states. Since then we have greatly expanded the experimental data base of disulfane with the particular aims of deriving a more precise potential function and a full substitution structure. Measurements of the pure rotational spectrum of HSSH in the millimeter-wave region have been extended to include many more transitions in the first excited torsional state ( $v_t = 1$ ) and, for the first time, transitions in the second excited ( $v_t = 2$ ) torsional state; in particular we have measured  $K = 1 \leftarrow 0$   $P$ -,  $Q$ -, and  $R$ -branch transitions and  $K = 2 \leftarrow 1$   $Q$ -branch transitions in  $v_t = 1$  and  $K = 1 \leftarrow 0$   $Q$ -branch transitions in  $v_t = 2$ . Details of much of this work along with isotopic studies will be published in a forthcoming paper concerning the substitution structure of disulfane, with the SSH bond angle determined for the first time from millimeter-wave data.

In addition to the newly measured pure rotational transitions, we have recently measured the infrared torsional-rotational spectrum of HSSH to high resolution on

the Fourier transform instrument at Giessen. Previous measurements of the torsional spectrum of HSSH were reported at low resolution, which was insufficient for an accurate determination of the torsional potential function (5-7). It is one purpose of this paper to present our new infrared results, which comprise several thousand rotationally analyzed lines involving the torsional transitions  $\nu_t = 1 \leftarrow 0$ ,  $2 \leftarrow 1$ , and  $3 \leftarrow 2$ . The new high-resolution infrared data led to the assignment of the  $\nu_t = 2$   $K = 1 \leftarrow 0$   $Q$ -branch rotational transitions, the band center of which lies in the millimeter region near 138.4 GHz.

The infrared transition wavenumbers have been fitted using a simple asymmetric top model in which different rotational and centrifugal distortion constants are determined for the torsional substates and the torsional splittings in the limit of zero rotation are treated as adjustable parameters. Such a treatment is viable because of the small interaction between overall rotational and torsional motions. The analyzed infrared lines are listed in Table I. Table II contains the vibrational energies and torsional splittings of the first four torsional states of HSSH. Torsional splittings for  $\nu_t = 2$  and 3 and vibrational energies of all states through  $\nu_t = 3$  have been determined from our analysis of the IR data whereas splittings for  $\nu_t = 0, 1$ , and 2 are from millimeter-wave data (1, 11). The newly assigned  $\nu_t = 2$   $K = 1 \leftarrow 0$   $Q$ -branch rotational transitions are listed in Table III.

The torsional splittings in  $\nu_t = 0, 1, 2$  and the band centers of the torsional transitions  $\nu_t = 1 \leftarrow 0$  and  $2 \leftarrow 1$  have been used to determine a refined torsional potential, shown in Fig. 1. The applicability of this potential has been tested by predicting the torsional splitting and energy of the  $\nu_t = 3$  state and has been found to be satisfactory.

TABLE II  
Energies of Torsional States in HSSH

Torsional State $\nu_t$	Energy ( $\text{cm}^{-1}$ ) <sup>a</sup>		Torsional Splittings (MHz)			
	Expt	Fit <sup>b</sup>	$1/2 [\Delta(4-1) + \Delta(3-2)]^c$		$1/2 [\Delta(4-1) - \Delta(3-2)]$	
			Expt.	Fit <sup>d</sup>	Expt.	Fit <sup>d</sup>
0	0	0	0.058(4) <sup>d</sup>	0.069	---	0.006
1	417.476765(7)	416.7	7.995(25) <sup>d</sup>	7.642	---	0.359
2	808.019808(12)	808.0	376.14(05) <sup>e</sup> 379.91 (81)	376.360	± 9	9.592
3	1171.406195(56)	1170.6	10642.7(3.3)	10602	135(18)	152.

<sup>a</sup> Energies relative to ground state; calculated zero-point energy of  $214.6 \text{ cm}^{-1}$

<sup>b</sup> Torsional splittings averaged. See text for discussion of analysis.

<sup>c</sup> Based on torsional potential derived from  $\nu_t = 0, 1, 2$  data.

<sup>d</sup> See theory section for discussion of the meaning of  $\Delta$

<sup>e</sup> Previously taken millimeter-wave data - see references (1, 11)

<sup>e</sup> Millimeter-wave data; present work.

TABLE III  
Measured Line Frequencies of the Second Excited ( $\nu_t = 2$ ) Torsional State of HSSH

J	lower component (MHz)	upper component (MHz)
1	138095.629	
2	138073.778	138825.514
3	138041.238	138793.068
4	137997.752	138749.828
5	137943.386	
6	137878.190	138630.928
7		138555.326
8	137715.280	
9		138371.803
10	137509.130	138263.982
11	137389.818	138145.432
12	137259.807	138016.195
13	137119.149	137876.393
14	136967.700	137725.844
15	136805.557	137564.682
16	136632.769	137392.910
17	136449.357	137210.606
18	136255.353	137017.768
19	136050.779	136814.439
20	135835.675	136600.658
21	135610.104	136376.445
22	135374.053	136141.848
23	135127.608	135896.917
24		135641.709

The remainder of this paper is organized as follows: in Section II, some experimental details and new spectra are presented. In Section III, the details of the theory of the torsional splittings in HSSH are reviewed and our analysis procedure detailed. Our results and conclusions are discussed in Section IV.

## II. EXPERIMENTAL DETAILS

The infrared and millimeter-wave data presented in this paper have been obtained with two spectrometers. The Bruker IFS 120 HR vacuum Michelson interferometer in Giessen was used to record the torsional-rotational bands of HSSH with an unapodized resolution of  $0.0018 \text{ cm}^{-1}$  (50 MHz). The bands encompass a spectral region from 300 to  $550 \text{ cm}^{-1}$ . The spectrum was calibrated using lines of the OCS  $\nu_2$  band reported by Jolma *et al.* (12). Experimental details of the interferometer have been discussed by Plummer *et al.* (10). There are several minor differences in the present measurement because of the different wavenumber region probed. The detector employed was a Ge-Cu type, the radiation source was a globar, the beam splitter was mylar of  $2.5 \mu\text{m}$  thickness, and the windows were of cesium iodide (CsI). The cell length was 2.80 m.

In Fig. 2 we present a small part of the torsional-rotational spectrum of HSSH. The selected region shows particularly clearly the torsional doubling associated with the  $\nu_t = 2 \leftarrow 1$  transitions. It may be pointed out that the assignment of these hot-band transitions led finally to the location of the  ${}^{\prime}Q_0$ -branch of the pure rotational

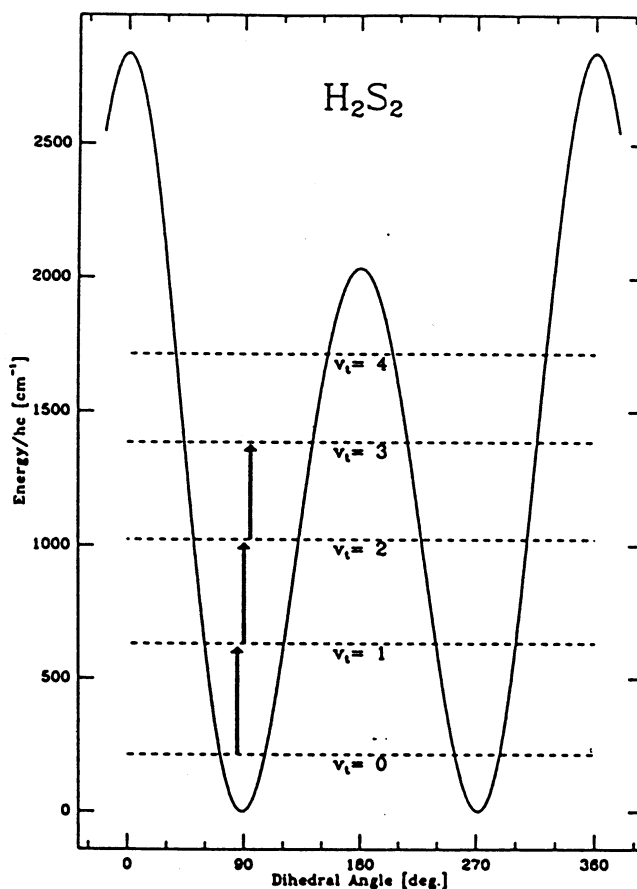


FIG. 1. The potential function  $V(x)$  is plotted as a function of the dihedral (torsional) angle  $x$ . The function is derived from the torsional splittings and band centers for  $v_t \leq 2$ . The torsional energy levels have been superimposed on the potential; torsional splittings are too small to be depicted. Bold arrows show the observed transitions.

transitions in the  $v_t = 2$  excited state. These transitions had not been seen in earlier  $Q$ -branch analyses (1-3) due to their relative weakness and the large size of the torsional splitting. Figure 3 illustrates some low  $J$  pure rotational  $Q_0$ -branch transitions and their splittings for both the  $v_t = 1$  and 2 torsional states of HSSH.

The millimeter-wave data were recorded with the computer-controlled millimeter-wave spectrometer in Cologne which employs a digital phase-sensitive detector; details of this spectrometer have been reported recently (13).

### III. THEORY AND ANALYSIS

In the internal axis method (IAM) pioneered by Hunt *et al.* (14) for molecules of the HSSH/HOOH class, the torsional motion can be separated from the rigid body rotational motion to a large extent. In this approach, the torsional levels are obtained by solution of the eigenvalue equation

$$\{F_T P_x^2 + V(x)\} \psi(x) = E \psi(x), \quad (1)$$

where  $x$  is the dihedral angle between the H-S groups,  $P_x$  is the torsional angular momentum,  $V(x)$  is the torsional potential, and  $F_T$  is the reduced rotational "constant" for torsional motion which, in reality, contains a small dependence on  $x$ . The  $P_x$

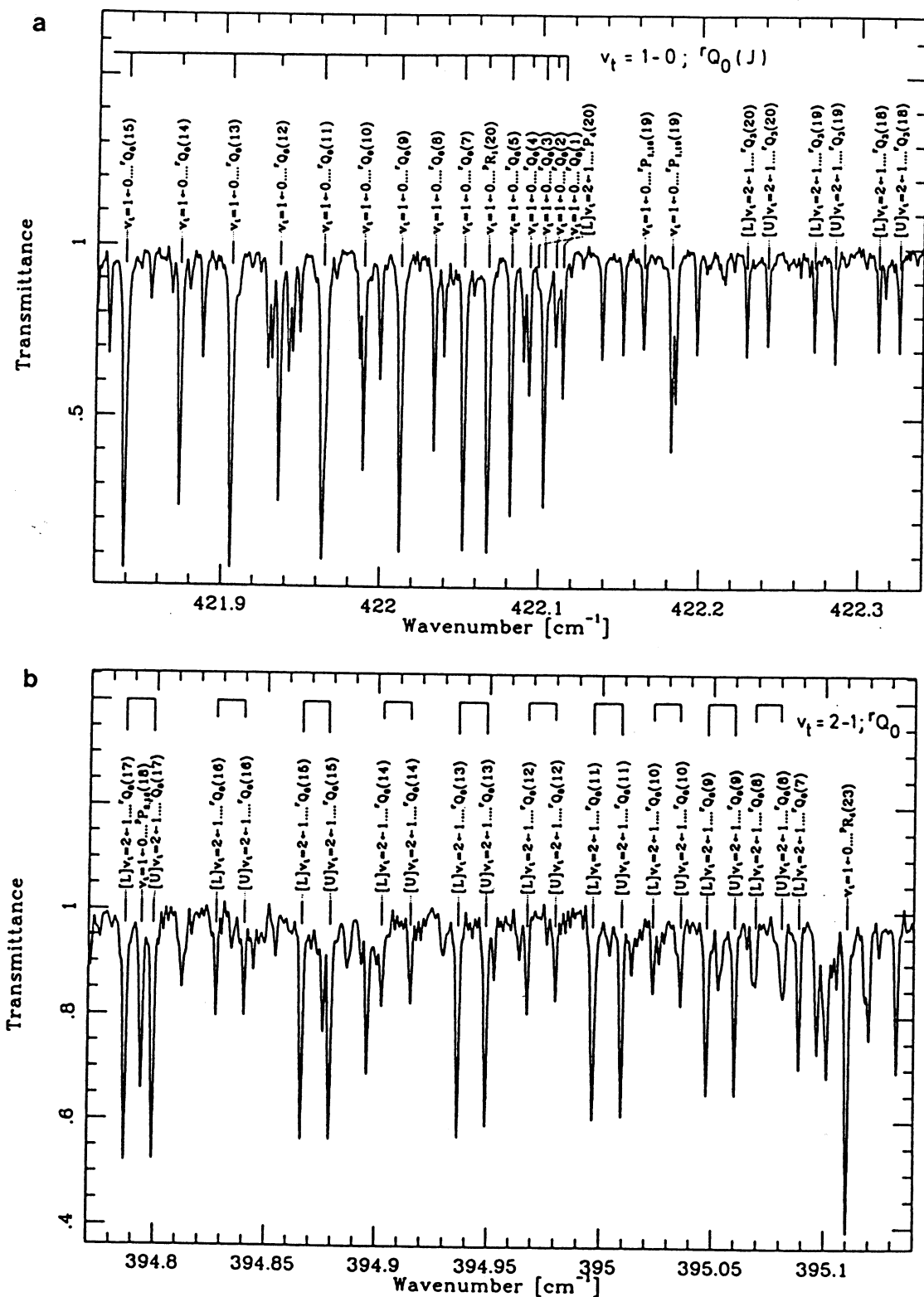


FIG. 2. (a) The torsional-rotational infrared spectrum near the band origin of the  $\nu_t = 1 \leftarrow 0$  band is depicted. The dominant features belong to the  ${}^rQ_0$  branch. (b) The torsional-rotational infrared spectrum near the band origin of the  $\nu_t = 2 \leftarrow 1$  band is depicted. The torsionally split lines are denoted by [L] and [U] for lower and upper, respectively. (c) The torsional-rotational infrared spectrum near the band origin of the  $\nu_t = 3 \leftarrow 2$  band is depicted. The torsionally split lines are once again denoted by [L] and [U].

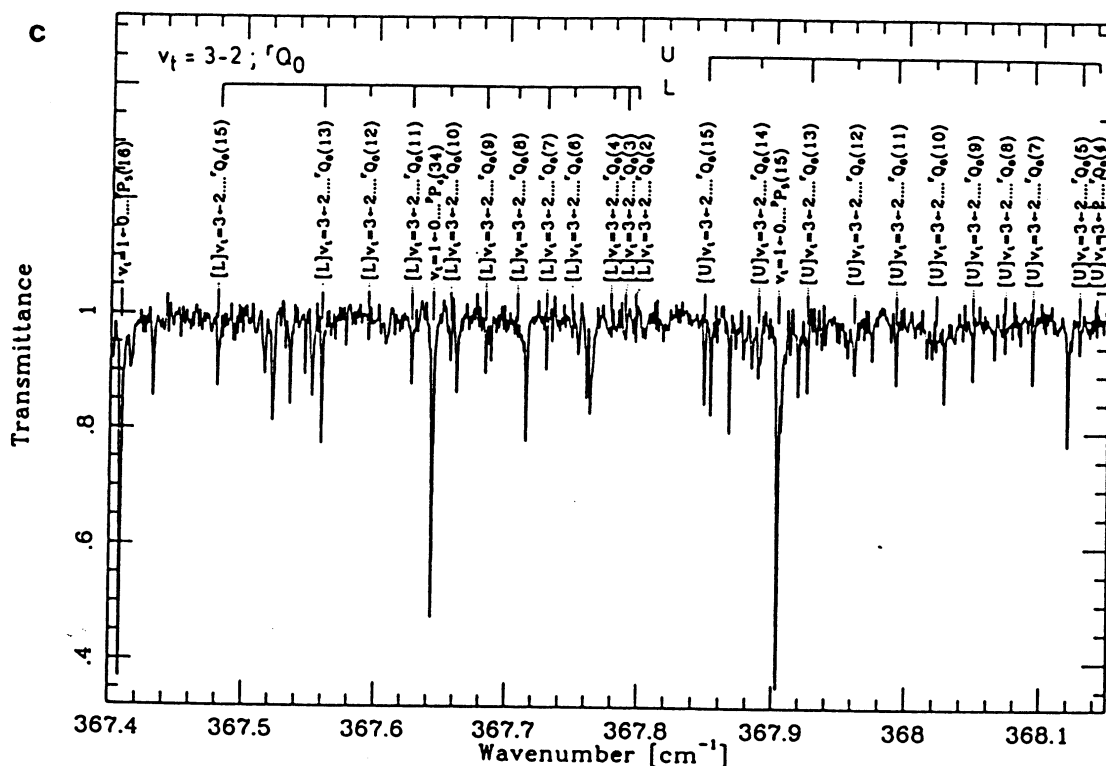


FIG. 2—Continued

operator used in (1) is only an approximate form of an operator which contains a small  $K$  dependence (14). The coordinate  $\chi$  is so chosen that angular motion of the two H-S groups preserves the direction of the axis that bisects the torsional angle. This axis is both an inertial axis of the molecule (either the  $b$  axis or the  $c$  axis depending upon the value of  $\chi$ ) and the axis along which the dipole moment points. With this definition for torsional motion, it is easily seen that one complete torsional period requires a range for  $\chi$  of  $0 \leq \chi \leq 4\pi$  rather than the more customary  $0 \leq \chi \leq 2\pi$ .

The torsional potential energy  $V(\chi)$  can be represented by a trigonometric expansion of the type

$$V(\chi) = V_0 + \sum_i V_i \cos(i\chi), \quad (2)$$

where  $V_0$  is defined so as to make the potential minima zero. For HSSH (as well as HOOH), where the minimum energy is neither at the *cis* position ( $\chi = 0, 2\pi, 4\pi, \dots$ ) nor at the *trans* position ( $\chi = \pi, 3\pi, \dots$ ) but close to the *gauche* form ( $\chi = \pi/2, 3\pi/2, \dots$ ), it is convenient to retain only the first three terms ( $V_1, V_2$ , and  $V_3$ ) in the cosine expansion. These terms are sufficient to reproduce the main features of the torsional potential, including barrier heights at the *cis* and *trans* positions which can differ from one another. Solution for Eq. (1) leads to torsional energy levels which are functions of  $F_T$  and the potential parameters.

The torsional energy levels are conveniently obtained with the use of orthonormal free-rotor basis functions  $(4\pi)^{-1/2} \exp(is\chi)$ , where  $s$  is any integer or half-integer due





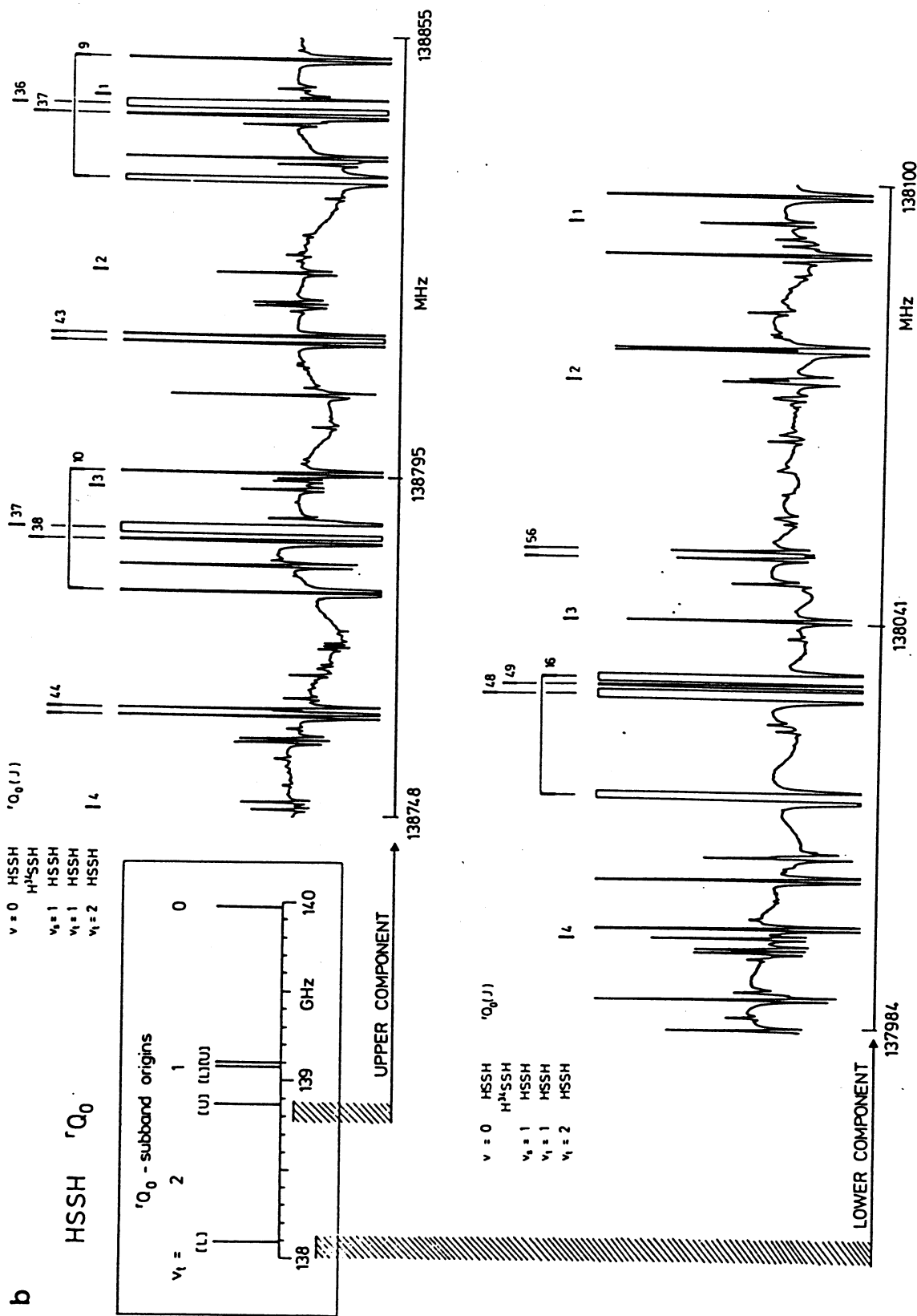


FIG. 3—Continued

to the range of  $\chi$ . Since the Hamiltonian operator connects only those basis functions with  $\Delta s = 0, \pm 1, \pm 2, \pm 3$ , the basis functions can be separated into two classes of the type  $(4\pi)^{-1/2} \exp[i(n + \sigma)\chi]$ , where  $n$  is an integer and  $\sigma = 0$  or  $\frac{1}{2}$ . In the calculations performed here the range of  $n$  has been limited to  $-20 \leq n \leq 20$ . Upon performance of the two distinct matrix diagonalizations, it is found that for  $\sigma = 0$ , the energy level pattern consists of closely spaced doublets which can be characterized by a joint quantum number  $v_t = 0, 1, 2, 3, \dots$ . The doublet splitting increases rapidly with increasing  $v_t$ . A similar pattern holds for the  $\sigma = \frac{1}{2}$  case, the only difference being a smaller doublet splitting than for the  $\sigma = 0$  case for each value of  $v_t$ . For states significantly below the potential barriers, the  $\sigma = 0$  and  $\sigma = \frac{1}{2}$  doublets have essentially the same center of gravity. Hunt *et al.* (14) have characterized the quartet of levels for each  $v_t$  by the additional quantum number  $\tau = 1, 2, 3, 4$  in the order of ascending energy so that  $\tau = 1$  and 4 refer to the  $\sigma = 0$  levels and  $\tau = 2$  and 3 refer to the  $\sigma = \frac{1}{2}$  levels. We maintain this convention throughout this paper. The eigenvectors  $\psi_{v_t, \tau}(\chi)$  corresponding to these four levels are symmetric and antisymmetric linear combinations of the exponential basis functions, so they can be expanded in trigonometric (cos or sin) series with terms of the type  $\cos(n\chi)$ ,  $\sin[(n + \frac{1}{2})\chi]$ ,  $\cos[(n + \frac{1}{2})\chi]$ , and  $\sin(n\chi)$  for  $\tau = 1, 2, 3, 4$ , respectively. The torsional wave functions  $\psi_{v_t, \tau}(\chi)$  can be characterized by the irreducible representations of the symmetry group of the torsional Hamiltonian (15, 16). In the approach of Dreizler (15), four symmetry elements are used to characterize this group, which is isomorphic with the well-known  $C_{2v}$  group. The symmetry elements are  $E$  ( $\chi \rightarrow \chi$  or  $\chi \rightarrow \chi + 4\pi$ ),  $T$  ( $\chi \rightarrow \chi + 2\pi$ ),  $\sigma_{trans}$  ( $\chi \rightarrow 2\pi - \chi$ ), and  $\sigma_{cis}$  ( $\chi \rightarrow 4\pi - \chi$ ). The character table is shown in Table IV. The four torsional wave functions for each  $v_t$  have the irreducible representations  $A_1$  ( $\tau = 1$ ),  $B_1$  ( $\tau = 2$ ),  $B_2$  ( $\tau = 3$ ), and  $A_2$  ( $\tau = 4$ ). To characterize the overall rotational-torsional wave functions in the approach of Dreizler (15) requires use of a direct product group of 16 elements made up of the torsional group and the well-known four-group  $V(a, b, c)$  for rigid asymmetric tops (17). In the extended permutation-inversion group approach utilized by Hougen (16) and Bunker (18), only eight elements are needed to characterize the torsional and rotational wave functions using a group designated  $G_4^\dagger$  or  $G_4(EM)$ . With Bunker's notation, the torsional wavefunctions have the irreducible representations  $A_{1s}$  ( $\tau = 1$ ),  $A_{2d}$  ( $\tau = 2$ ),  $A_{1d}$  ( $\tau = 3$ ), and  $A_{2s}$  ( $\tau = 4$ ), where the subscripts  $s$  and  $d$  refer to the single- or double-group representations. The character table for this extended group is contained in Table V.

TABLE IV  
Character Table for Dreizler's Torsional Group  $L$

L	E	T	$\sigma_t$	$\sigma_c$	
$A_1$	1	1	1	1	$\cos n\chi$ ( $\tau = 1$ )
$A_2$	1	1	-1	-1	$\sin n\chi$ ( $\tau = 4$ )
$B_1$	1	-1	1	-1	$\sin(n + 1/2)\chi$ ( $\tau = 2$ )
$B_2$	1	-1	-1	1	$\cos(n + 1/2)\chi$ ( $\tau = 3$ )

TABLE V

Character Table for Extended Permutation-Inversion Group

$G_4^*$	E	P	P*	E*	T	PT	PT*	T*	$K_a K_c$
$A_{1s}$	1	1	1	1	1	1	1	1	$\cos n\lambda$ ( $\tau=1$ ) e e
$A_{2s}$	1	1	-1	-1	1	1	-1	-1	$\sin n\lambda$ ( $\tau=4$ )
$B_{1s}$	1	-1	1	-1	1	-1	1	-1	e o
$B_{2s}$	1	-1	-1	1	1	-1	-1	1	
$A_{1d}$	1	1	1	1	-1	-1	-1	-1	$\cos (n \cdot 1/2)\lambda$ ( $\tau=3$ )
$A_{2d}$	1	1	-1	-1	-1	-1	1	1	$\sin (n \cdot 1/2)\lambda$ ( $\tau=2$ ) o e
$B_{1d}$	1	-1	1	-1	-1	1	-1	1	
$B_{2d}$	1	-1	-1	1	-1	1	1	-1	o o

Definition of operations: E - Identity, P - permutation (12)(ab) where molecular framework is  $\begin{matrix} H & S & S & H \\ 1 & a & b & 2 \end{matrix}$ , (E)\* - inversion, T - Increase torsional angle by  $2\pi$

The spacings among the quartet of levels for each  $v_t$  are quite sensitive to the *cis* and *trans* barrier heights. A simple treatment of the torsional eigenvalue problem using harmonic oscillator-like (localized) basis functions rather than the free-rotor functions utilized in our treatment shows this effect nicely (16). For the case of HSSH, in which the *cis* barrier height ( $V_{cis}$ ) is significantly greater than the *trans* barrier height ( $V_{trans}$ ), the energy level pattern is such that the  $\tau = 1$  and 2 levels are very closely spaced, as are the  $\tau = 3$  and 4 levels. Indeed, as  $V_{cis}$  becomes much larger than  $V_{trans}$ , the two pairs of levels become degenerate and the  $\sigma = 0$  doublet spacing  $\Delta(4 - 1)$  equals the  $\sigma = \frac{1}{2}$  doublet spacing  $\Delta(3 - 2)$ . On the other hand, as  $V_{cis}$  is reduced in size to approach  $V_{trans}$ ,  $\Delta(3 - 2)$  becomes significantly smaller than  $\Delta(4 - 1)$ . Thus the difference in splittings  $\frac{1}{2}[\Delta(4 - 1) - \Delta(3 - 2)]$  is mainly a measure of  $V_{cis}$ . If  $V_{cis}$  is fixed and  $V_{trans}$  varied, then both  $\Delta(4 - 1)$  and  $\Delta(3 - 2)$  vary dramatically although their difference is fairly constant. Thus, the average splitting  $\frac{1}{2}[\Delta(4 - 1) + \Delta(3 - 2)]$  is mainly a measure of  $V_{trans}$ .

Although the discussion up to this point has given the impression that torsional motion produces a quartet of closely spaced levels for each state characterized by  $v_t$ , the proper inclusion of rigid-body rotational motion reduces the number of states by a factor of two (14-16). This reduction stems from the fact that the overall rotational-torsional wave functions must be characterized by single-group representations in the  $G_4(EM)$  group. The asymmetric rotor eigenfunctions  $|J, K_a, K_c\rangle$  transform as single-group representations if  $K_a$  is even and as double-group representations if  $K_a$  is odd. Thus if  $K_a$  is even, the only allowed torsional states are those with single-group representations ( $\tau = 1, 4$ ), whereas if  $K_a$  is odd, the only allowed torsional states are those with double-group representations ( $\tau = 2, 3$ ). Both the allowed torsional levels (regular lines) and the unallowed levels (dotted lines) are shown in Fig. 4 for low values of  $K_a$  (referred to as  $K$  in the figure).

The torsional selection rules for spectroscopic transitions are also easily obtained via group theory. The dipole moment of the molecule can be written as

$$\mu = \mu_i \cos(\chi/2), \quad (3)$$

where  $i$  stands for the inertial axis, which for HSSH is the  $c$ -axis. Since  $\cos(\chi/2)$  transforms as  $A_{1d}$  in the  $G_4(EM)$  group, the allowed torsional transitions are  $A_{1s} \leftrightarrow A_{1d} (\tau = 1 \leftrightarrow 3)$  and  $A_{2s} \leftrightarrow A_{2d} (\tau = 4 \leftrightarrow 2)$ . In the approach of Dreizler (15),  $\cos(\chi/2)$  transforms as  $B_2$ , and the allowed torsional transitions are  $A_1 \leftrightarrow B_2 (\tau = 1 \leftrightarrow 3)$  and  $A_2 \leftrightarrow B_1 (\tau = 4 \leftrightarrow 2)$ . Group theory yields no limiting selection rules for  $\Delta v_t$ ; however, the large *cis* and *trans* barriers for HSSH and the resultant small splittings caused by torsional motion indicate that harmonic oscillator selection rules ( $\Delta v_t = \pm 1$ ) are applicable, a result we have confirmed by intensity calculations. For example, we calculate that the  $v_t = 2 \leftarrow 0, \tau = 3 \leftarrow 1$  transition has a transition dipole only  $\approx 10\%$  of that of the fundamental transition.

The rotational transitions are  $c$ -type ( $\Delta J = 0, \pm 1; \Delta K_a = \text{odd}$ ). Figure 4 shows some strongly allowed ( $\Delta K_a = 1$ ) transitions for both millimeter-wave ( $\Delta v_t = 0$ ) and far-infrared ( $\Delta v_t = 1$ ) radiation. It can be seen that the torsional splittings  $\Delta\nu$  in the millimeter-wave lines are given by the sum of  $\Delta(4-1)$  and  $\Delta(3-2)$ . The millimeter-

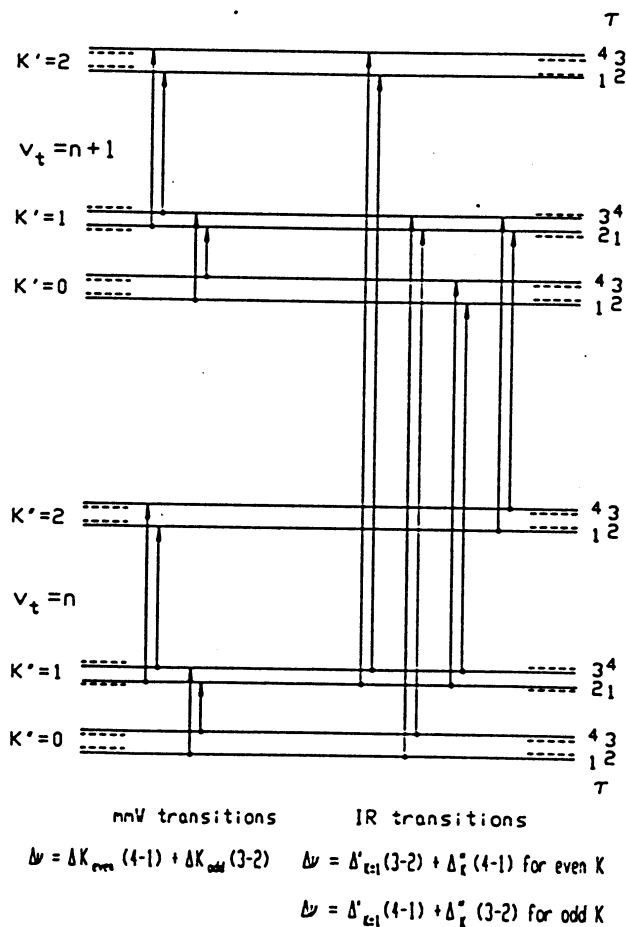


FIG. 4. The allowed torsional-rotational levels and transitions are shown for low  $K$  values. Single and double primes in the expressions for the torsional splittings  $\Delta\nu$  refer to the upper and lower torsional levels, respectively. Note that the torsional splittings seen in the pure rotational, millimeter-wave (mmW) spectrum only determine the sum of the  $\tau = 4-1$  and  $\tau = 3-2$  splittings in a given torsional state.

wave splittings therefore cannot be used to decouple  $\Delta(4 - 1)$  from  $\Delta(3 - 2)$  if they do not depend on  $K_a$ ; these splittings yield information concerning  $V_{trans}$  but not  $V_{cis}$ , as discussed above. For the IR data, on the other hand, the splittings are given by  $\Delta''(4 - 1) + \Delta'(3 - 2)$  and  $\Delta''(3 - 2) + \Delta'(4 - 1)$ , where ' refers to the upper  $v_t$  state and '' to the lower  $v_t$  state and the two expressions refer to  $K_a''$  even and odd ( $K_a'$  odd and even), respectively. Since the splitting of the upper state is much larger than that of the lower state and since  $\Delta(4 - 1)$  exceeds  $\Delta(3 - 2)$  by an amount related to the size of the *cis* barrier, any small alternation in torsional splitting observed in the IR as  $K_a''$  varies between even and odd values is sensitive to the difference between  $\Delta'(4 - 1)$  and  $\Delta'(3 - 2)$  and yields direct information on  $V_{cis}$  (16). Such alternation is large enough to be seen in the  $v_t = 3 \leftarrow 2$  IR spectrum.

In a previous communication on HSSH (11), we utilized a weighted nonlinear least-squares fit to the millimeter-wave data on the lowest  $J$  torsional splittings in  $v_t = 0$  and 1, preliminary IR data on the band centers for  $v_t = 1 \leftarrow 0$  and  $2 \leftarrow 1$ , and the IR-determined torsional splitting in  $v_t = 2$  to obtain a potential function for torsional motion of the type shown in Eq. (2) with terms through  $V_3$ . We then determined  $V_{cis}$  and  $V_{trans}$  to be  $(2800 \pm 90) \text{ cm}^{-1}$  and  $(1990 \pm 15) \text{ cm}^{-1}$ , respectively, with the major uncertainty caused by a lack of knowledge of  $F_T$ . (Without the IR band centers,  $V_{cis}$  could not have been determined, since the millimeter-wave torsional splittings by themselves are not sensitive to this barrier.) The values for  $V_{cis}$  and  $V_{trans}$  are in excellent agreement with the results of previous ab initio quantum chemical calculations (19, 20) which show, however, that as the torsional motion occurs, other changes occur in the skeletal framework of the molecule, particularly in the S-S bond length and the SSH angle. The reduced rotational "constant"  $F_T$  could not be obtained in our least-squares fit and had to be calculated based on an oversimplified model in which the skeletal framework of the molecule remains rigid except for the torsional motion (14). Although there is a dependence of  $F_T$  on  $\chi$  to consider in this model, a larger problem was a discrepancy between the previous experimental (1, 8) and ab initio theoretical (19, 20) values for the SSH bond angle. This discrepancy has now been resolved in favor of the theoretically determined angle (see Section IV). Using our new  $r_0$  structure (to be presented and refined in a forthcoming paper), we have recalculated the  $\chi$ -independent part of  $F_T$  to be  $19.61 \text{ cm}^{-1}$ . It makes little sense to include the small  $\chi$ -dependent terms in  $F_T$  in a solution of the torsional problem because the model on which they are based (a rigid skeleton) is not valid. Using the value of  $F_T$  newly obtained, including the new  $v_t = 2$  low  $J$  torsional splitting measured accurately in our millimeter-wave apparatus, and changing the weights of our previous fit slightly to emphasize the torsional splittings over the IR band centers (see below), we have refitted the torsional data. The results of the fit can be seen in Table II. They are discussed in the next section along with the potential function determined. Figure 1 contains the torsional potential function and the torsional levels.

The success of the IAM treatment in understanding the torsional splittings in the torsional-rotational spectrum of HSSH suggests that this approach should be used to fit all of the measured transition frequencies. Such an approach has been utilized for methanol and similar three-fold internal rotors (21). In this treatment, the torsional wave functions and symmetric or asymmetric top rotational functions are multiplied together and used as basis functions to diagonalize a Hamiltonian matrix containing torsional, rotational, and rotational-torsional interaction terms. Although this method

is indispensable for methanol, in which the rotational-torsional interaction is large even with the IAM Hamiltonian specifically designed to reduce it, the small rotational-torsional interaction seen in HSSH suggests a more empirical and simpler approach used previously to study the millimeter-wave spectrum of HOOH (22) as well as in earlier papers on HSSH (1-3, 10). In this approach, the torsional-rotational spectrum is fitted to a Watson-type  $S$ -reduced asymmetric top Hamiltonian in which all  $v_t$ ,  $\tau$  states are accorded their own sets of rotational constants (if necessary) and the torsional energies and splittings in the absence of rotation are treated as adjustable parameters. Any small torsional-rotational interaction is absorbed in the differing rotational and centrifugal distortion constants. The reason rotational-torsional interaction is so much larger in methanol than in HOOH or HSSH has to do with the different symmetries of the molecules and has been discussed by Hunt *et al.* (14).

#### IV. DISCUSSION OF RESULTS

As discussed in Section III, the transition wavenumbers in Table I have not been analyzed by the IAM approach with the inclusion of torsional-rotational interaction (14) but by a simpler method in which different rotational and centrifugal distortion constants are utilized for the different torsional substates. The torsional energies and  $v_t = 2, 3$  torsional splittings determined by this method are contained in the "experimental" columns of Table II. The  $v_t = 2$  "symmetric" torsional splitting ( $\frac{1}{2}[\Delta(4-1) + \Delta(3-2)]$ ) so deduced of  $379.91 \pm 0.81$  MHz compares well with the millimeter-wave value of  $376.14 \pm 0.05$  MHz. The spectroscopic parameters determined by this approach are shown in Table VI. Not all of the infrared data could be analyzed by our procedure; higher  $J$  and  $K_a$  states are significantly affected by Coriolis coupling (see below) and are excluded from the current data set.

Although the substitution structure for disulfane will be reported in a future publication, the HSS bond angle merits special discussion here due to a previous substantial discrepancy between experimental and theoretical values. The experimentally determined value for  $\angle$ SSH was originally reported to be  $91-92^\circ$  (1, 8) based partially on electron diffraction work. More recent *ab initio* treatments have obtained a value of  $98.4^\circ$  (19, 20). Our current  $r_0$  structure is in substantial agreement with the theoretical treatments; we obtain  $99.4^\circ$  for  $\angle$ SSH.

Our new fit to the torsional data for  $v_t \leq 2$  results in refined values for  $V_{cis}$  and  $V_{trans}$  of  $2843 \pm 9$   $\text{cm}^{-1}$  and  $2037 \pm 12$   $\text{cm}^{-1}$  based on the directly determined parameters  $V_1 = 274 \pm 5$   $\text{cm}^{-1}$ ,  $V_2 = 1219 \pm 5$   $\text{cm}^{-1}$ , and  $V_3 = 129 \pm 12$   $\text{cm}^{-1}$ . The errors are  $1\sigma$  deviations obtained under the assumption that  $F_T$  is known exactly. True uncertainties are clearly larger. The potential function minimizes at a torsional angle  $\chi$  of  $89^\circ$  which is reasonably close to the experimental  $r_0$  angle of  $90.54^\circ$ . The results in Table II show that the torsional splittings of HSSH are well determined by a simple potential of the type shown in Eq. (2). Using just three potential parameters ( $V_1$ ,  $V_2$ , and  $V_3$ ), we have been able to fit the highly accurate low  $J$  torsional splittings for  $v_t = 0, 1, 2$  determined from the pure rotational spectrum of HSSH with residuals (observed - calculated) of  $-0.11, 0.35,$  and  $-0.12$  MHz for  $v_t = 0, 1, 2$ , respectively, as well as the band centers for the  $v_t = 1 \leftarrow 0$  and  $2 \leftarrow 1$  transitions. Somewhat larger than the experimental precision, the residuals for the torsional splittings reflect the simplicity of the potential function and the one-dimensional treatment. In the fit

TABLE VI  
 Effective Spectroscopic Parameters<sup>a</sup>

Constant	Ground state <sup>b</sup>	$v_t=1$
A /MHz	146858.1473(46)	146038.013(61)
B /MHz	6970.42953(62)	6942.6302(29)
C /MHz	6967.68832(61)	6931.6476(29)
D <sub>J</sub> /kHz	5.39762(44)	5.38755(152)
D <sub>JK</sub> /kHz	85.4059(70)	87.551(112)
D <sub>K</sub> /MHz	2.427270(54)	2.3165(55)
d <sub>1</sub> /Hz	9.015(22)	-0.08339(27)
d <sub>2</sub> /Hz	-27.2244(72)	-30.16(73)
H <sub>J</sub> /Hz	-0.001517(104)	0.0(fixed)
H <sub>JK</sub> /Hz	-0.0549(24)	0.0(fixed)
H <sub>KJ</sub> /Hz	1.629(23)	-57.4(43)
H <sub>K</sub> /kHz	0.100986(118)	0.172(142)
E(v)-E(v-1) /cm <sup>-1</sup>	—	417.4767646(66)

Constant	$v_t=2$ (lower)	$v_t=2$ (upper)
A /MHz	145392.321(146)	145388.606(149)
B /MHz	6917.0241(78)	6916.9684(81)
C /MHz	6895.6815(80)	6895.7727(81)
D <sub>J</sub> /kHz	5.3726(36)	5.3804(36)
D <sub>JK</sub> /kHz	103.99(24)	103.23(27)
D <sub>K</sub> /MHz	2.4342(126)	2.0216(127)
d <sub>1</sub> /Hz	-21.8(71)	36.0(80)
d <sub>2</sub> /Hz	-50.55(174)	-45.33(155)
H <sub>KJ</sub> /Hz	-283.3(93)	-321.6(98)
H <sub>K</sub> /kHz	4.72(31)	-6.89(32)
E(v)-E(v-1) /cm <sup>-1</sup>	390.5365737(183)	390.5495127(197)

Constant	$v_t=3$ (lower)	$v_t=3$ (upper)
A /MHz	144783.26(87)	144779.37(100)
B /MHz	6892.362(26)	6892.191(28)
C /MHz	6857.083(25)	6857.848(29)
D <sub>J</sub> /kHz	5.396(21)	5.393(24)
D <sub>JK</sub> /kHz	84.8(26)	89.9(25)
D <sub>K</sub> /MHz	0.0(fixed)	0.0(fixed)
d <sub>1</sub> /Hz	-6.3(217)	-4.6(226)
d <sub>2</sub> /Hz	-78.1(88)	-65.8(61)
E(v)-E(v-1) /cm <sup>-1</sup>	363.202549(66)	363.570224(87)
E <sub>cis</sub>   /MHz <sup>c</sup>	72.7(130)	62.4(130)

<sup>a</sup>Numbers in parentheses are one standard deviations.

<sup>b</sup>Revised constants. See also Ref.(10).

<sup>c</sup>The value of  $[\Delta(4-1) - \Delta(3-2)]/2$  in Table II is obtained by adding these values of upper and lower component. Errors for this constant were estimated by manual adjustments.

reported here (but not in the preliminary version of Ref. (11)), the band centers have been assigned a weight corresponding to an uncertainty of 0.05 cm<sup>-1</sup>, significantly greater than their deduced uncertainties, because it is clear that the band centers are influenced to some degree by Fermi-type (potential) coupling involving the low-lying (510-cm<sup>-1</sup>) first excited S-S stretching state ( $v_s = 1$ ). A strong Coriolis coupling has

already been detected involving the  $v_t = 1$  and  $v_s = 1$  states in the high  $K_a$  FIR pure rotational spectrum. The potential coupling, to be discussed and analyzed in a future paper in which ab initio theory is used to determine its magnitude (23), involves mainly the  $v_t = 2$  state despite the fact that the energy for this state of  $808 \text{ cm}^{-1}$  places it farther from the first excited S-S stretching state ( $v_s = 1$ ) than the  $v_t = 1$  state, at  $417 \text{ cm}^{-1}$ , which is also connected to the  $v_s = 1$  state due to the large-amplitude nature of the torsional motion. The most obvious manifestation of the coupling is an abnormally large torsional splitting ( $\frac{1}{2}[\Delta(4 - 1) + \Delta(3 - 2)] \approx 0.5 \text{ MHz}$ ) in the  $v_s = 1$  state, seen many years ago but only recently explained (23). It can be seen in Table II that the fit to the torsional band centers results in vibrational energies that are only good to  $\approx 0.5 \text{ cm}^{-1}$ . A more accurate determination of the energy levels would require solution of at least a two-dimensional Schrodinger equation with coordinates for torsional motion and the S-S stretch, and possibly a multi-dimensional equation involving other low frequency motions as well. The low  $J, K$  torsional splittings in the  $v_t = 0, 1, 2, 3$  states, on the other hand, are not affected as greatly by the potential coupling.

The utility of the torsional potential determined from the data involving the  $v_t = 0, 1$ , and 2 states in predicting the  $v_t = 3$  state data is also shown in Table II. The symmetric rotationless torsional splitting  $\frac{1}{2}[\Delta(4 - 1) + \Delta(3 - 2)]$  is determined to be  $10\,642.7 \pm 3.3 \text{ MHz}$  from IR data whereas it is predicted to be  $10\,602 \text{ MHz}$  from the fit to the lower state data. This splitting is associated with the potential barrier  $V_{\text{trans}}$ . The asymmetric torsional splitting  $\frac{1}{2}[\Delta(4 - 1) - \Delta(3 - 2)]$  is measured to be  $135 \pm 18 \text{ MHz}$  and predicted to be  $152 \text{ MHz}$ . This latter splitting is associated with  $V_{\text{cis}}$ . That the predicted splittings differ somewhat from those measured is not too surprising given the large size of the  $v_t = 3$  splittings. Note that the splitting associated with  $V_{\text{cis}}$  was too small in the  $v_t \leq 2$  states to be seen in the IR torsional spectrum and cannot be detected at all in the pure rotational spectrum due to the selection rules. Yet the potential determined from the  $v_t \leq 2$  data was able to predict this splitting and determine the value of  $V_{\text{cis}}$  based primarily on the positions of the band centers for the  $v_t = 1 \leftarrow 0$  and  $2 \leftarrow 1$  transitions. Clearly the energies of the excited torsional states are sensitive to the entire potential function  $V(x)$ .

Although a full IAM treatment of the pure rotational and torsional-rotational spectra of HSSH is not needed to analyze the data set presented here, it might prove useful in further refining the torsional potential. In the case of methanol, a full IAM treatment did permit an accurate determination of the reduced rotational constant  $F_T$ . Were this parameter to be determined for HSSH, there would be even less uncertainty in the deduced torsional potential function.

## V. ACKNOWLEDGMENTS

We thank J. Behrend for help with the data processing, K. Lattner for help with the IR measurements, and B. Winnewisser for help in the preparation of this manuscript. E.H. acknowledges the support of the National Science Foundation via Grant CHEM-8515331 and thanks the Alexander von Humboldt Stiftung (Federal Republic of Germany) for making his stay in Cologne possible. The work in Cologne was supported by the Deutsche Forschungsgemeinschaft (Federal Republic of Germany) via Research Grant SFB-301. The work in Giessen was supported in part by the Deutsche Forschungsgemeinschaft and the Fond der Chemischer Industrie (Federal Republic of Germany).



TABLE I

Observed IR Transitions (in  $\text{cm}^{-1}$ ) of HSSH

J Ka Kc	- J Ka Kc	Observed	O-C	J Ka Kc	- J Ka Kc	Observed	O-C
v <sub>c</sub> - 1 - 0 Band							
25	1 24 - 26 0 26	409.40684	0.00001	10	2 9 - 11 1 11	426.14032	0.00000
24	1 23 - 25 0 25	409.91917	0.00003	10	2 8 - 11 1 10	426.13478	0.00002
23	1 22 - 24 0 24	410.42961	0.00000	9	2 8 - 10 1 10	426.62626	-0.00020
22	1 21 - 23 0 23	410.93809	-0.00013	9	2 7 - 10 1 9	426.62141	-0.00001
21	1 20 - 22 0 22	411.44499	0.00000	8	2 6 - 9 1 9	427.11009	0.00004
20	1 19 - 21 0 21	411.94991	-0.00001	7	2 6 - 8 1 8	427.10591	-0.00001
19	1 18 - 20 0 20	412.45309	0.00012	7	2 5 - 8 1 7	427.59154	-0.00003
18	1 17 - 19 0 19	412.95416	0.00000	5	2 3 - 6 1 5	427.58630	0.00003
17	1 16 - 18 0 18	413.45342	-0.00006	3	2 1 - 4 1 3	428.54658	0.00008
16	1 15 - 17 0 17	413.95092	0.00000	2	2 1 - 3 1 3	429.49609	0.00002
15	1 14 - 16 0 16	414.44647	-0.00002	25	2 23 - 25 1 23	430.96813	0.00000
14	1 13 - 15 0 15	414.94018	0.00001	25	2 24 - 25 1 24	430.66615	-0.00009
13	1 12 - 14 0 14	415.43197	0.00000	24	2 22 - 24 1 24	430.73667	-0.00008
12	1 11 - 13 0 13	415.92184	-0.00004	24	2 23 - 24 1 23	430.71160	0.00010
11	1 10 - 12 0 12	416.40994	0.00005	23	2 21 - 23 1 23	430.78912	-0.00004
10	1 9 - 11 0 11	416.89824	0.00003	23	2 22 - 23 1 22	430.76412	0.00004
9	1 8 - 10 0 10	417.38252	0.00000	22	2 20 - 22 1 22	430.83743	-0.00004
8	1 7 - 9 0 9	417.86135	0.00006	22	2 21 - 22 1 21	430.81448	0.00001
7	1 6 - 8 0 8	418.34296	-0.00002	21	2 19 - 21 1 21	430.88368	0.00000
6	1 5 - 7 0 7	418.82135	0.00000	20	2 18 - 20 1 20	430.92779	-0.00001
5	1 4 - 6 0 6	419.29792	0.00005	20	2 19 - 20 1 19	430.90671	-0.00001
4	1 3 - 5 0 5	419.77259	0.00003	19	2 17 - 19 1 19	430.96873	-0.00004
3	1 2 - 4 0 4	420.24327	0.00000	19	2 18 - 19 1 18	430.95231	-0.00001
2	1 1 - 3 0 3	420.71598	0.00000	18	2 16 - 18 1 18	431.00967	-0.00006
25	1 25 - 25 0 25	421.36313	-0.00004	18	2 17 - 18 1 17	430.99419	0.00003
23	1 23 - 23 0 23	421.47672	-0.00003	17	2 15 - 17 1 17	431.04731	-0.00004
22	1 22 - 22 0 22	421.53009	0.00003	17	2 16 - 17 1 16	431.03362	0.00001
21	1 21 - 21 0 21	421.58106	0.00000	16	2 14 - 16 1 16	431.08318	-0.00009
20	1 20 - 20 0 20	421.62962	0.00008	16	2 15 - 16 1 15	431.07082	-0.00005
19	1 19 - 19 0 19	421.67809	-0.00002	15	2 13 - 15 1 15	431.11687	-0.00001
18	1 18 - 18 0 18	421.72619	0.00004	15	2 12 - 14 1 14	431.10589	-0.00005
17	1 17 - 17 0 17	421.77487	-0.00001	14	2 12 - 14 1 14	431.14843	0.00003
16	1 16 - 16 0 16	421.80127	-0.00002	14	2 13 - 14 1 13	431.15882	0.00000
15	1 15 - 15 0 15	421.83838	0.00000	13	2 11 - 13 1 13	431.17779	-0.00003
14	1 14 - 14 0 14	421.87332	0.00016	13	2 12 - 13 1 12	431.16949	-0.00003
13	1 13 - 13 0 13	421.90561	0.00000	12	2 10 - 12 1 12	431.20513	0.00000
12	1 12 - 12 0 12	421.93586	0.00011	12	2 11 - 12 1 11	431.19602	0.00001
11	1 11 - 11 0 11	421.96360	0.00003	11	2 9 - 11 1 11	431.23034	-0.00001
10	1 10 - 10 0 10	421.98908	0.00000	11	2 10 - 11 1 10	431.22439	0.00007
9	1 9 - 9 0 9	422.01227	0.00001	10	2 8 - 10 1 10	431.25347	0.00001
8	1 8 - 8 0 8	422.03315	0.00002	10	2 9 - 10 1 9	431.24447	0.00003
7	1 7 - 7 0 7	422.05173	0.00006	9	2 7 - 9 1 9	431.27447	0.00000
6	1 6 - 6 0 6	422.06855	0.00004	8	2 6 - 8 1 8	431.29327	-0.00012
5	1 5 - 5 0 5	422.08342	0.00001	8	2 7 - 8 1 7	431.29009	-0.00001
4	1 4 - 4 0 4	422.09542	0.00005	7	2 5 - 7 1 7	431.31020	0.00000
3	1 3 - 3 0 3	422.10275	0.00013	7	2 6 - 7 1 6	431.30770	0.00006
2	1 2 - 2 0 2	422.10977	0.00013	6	2 4 - 6 1 6	431.32494	0.00003
1	1 1 - 1 0 1	422.11426	-0.00001	6	2 5 - 6 1 5	431.32302	0.00003
2	1 1 - 1 0 1	423.04044	-0.00014	5	2 3 - 5 1 5	431.33743	0.00008
3	1 2 - 2 0 2	423.49961	-0.00002	4	2 3 - 4 1 3	431.34718	0.00008
4	1 3 - 3 0 3	423.95674	0.00001	3	2 1 - 3 1 3	431.35625	-0.00018
5	1 4 - 4 0 4	424.41185	0.00000	2	2 1 - 2 1 1	431.36231	0.00005
6	1 5 - 5 0 5	424.86503	0.00003	2	2 1 - 1 1 1	432.29247	0.00000
7	1 6 - 6 0 6	425.31621	0.00004	2	2 0 - 1 1 0	432.29247	0.00009
8	1 7 - 7 0 7	425.76536	0.00001	3	2 2 - 2 1 2	432.75082	-0.00021
9	1 8 - 8 0 8	426.21263	0.00006	3	2 1 - 2 1 1	432.75082	0.00007
10	1 9 - 9 0 9	426.65779	0.00003	4	2 3 - 3 1 3	433.20733	-0.00014
11	1 10 - 10 0 10	427.10103	0.00005	4	2 3 - 4 1 3	433.66100	0.00012
12	1 11 - 11 0 11	427.54222	0.00003	5	2 5 - 5 1 5	434.11391	-0.00008
13	1 12 - 12 0 12	427.98137	-0.00003	6	2 5 - 6 1 6	434.56328	-0.00014
14	1 13 - 13 0 13	428.41859	-0.00001	7	2 5 - 6 1 5	435.01199	0.00010
15	1 14 - 14 0 14	428.85380	0.00001	8	2 7 - 7 1 7	435.00954	-0.00006
16	1 15 - 15 0 15	429.28697	0.00000	8	2 6 - 7 1 6	435.45777	0.00001
17	1 16 - 16 0 16	429.71813	0.00000	9	2 8 - 8 1 8	435.45452	0.00002
18	1 17 - 17 0 17	430.14721	-0.00005	10	2 9 - 9 1 9	435.89731	0.00018
19	1 18 - 18 0 18	430.59941	-0.00002	10	2 8 - 9 1 8	436.33814	0.00017
20	1 19 - 19 0 19	431.02245	0.00000	11	2 9 - 10 1 9	436.78241	0.00001
21	1 20 - 20 0 20	431.44344	0.00000	12	2 11 - 11 1 11	436.77631	-0.00002
22	1 21 - 21 0 21	431.86241	0.00003	13	2 12 - 12 1 12	437.21967	0.00004
23	1 22 - 22 0 22	432.26241	0.00001	13	2 11 - 12 1 11	437.21244	-0.00001
24	1 23 - 23 0 23	432.67928	0.00001	14	2 12 - 13 1 12	437.65470	-0.00001
25	1 24 - 24 0 24	433.09414	0.00003	14	2 13 - 13 1 13	437.64630	-0.00002
23	2 24 - 26 1 26	418.61280	0.00014	15	2 14 - 14 1 14	438.08762	0.00000
25	2 23 - 26 1 25	418.97975	-0.00006	15	2 13 - 14 1 13	438.07791	-0.00002
24	2 23 - 25 1 23	419.12860	0.00003	16	2 15 - 15 1 15	438.51840	0.00002
24	2 22 - 25 1 24	419.09621	0.00001	16	2 14 - 15 1 14	438.50720	-0.00009
23	2 22 - 24 1 24	419.64256	0.00009	17	2 16 - 16 1 16	438.94699	0.00002
23	2 21 - 24 1 23	419.61447	-0.00004	17	2 15 - 16 1 15	438.93439	0.00001
22	2 21 - 23 1 23	420.15445	0.00002	18	2 17 - 17 1 17	439.37342	0.00003
22	2 20 - 23 1 22	420.12867	-0.00005	18	2 16 - 17 1 16	439.35907	-0.00014
21	2 19 - 22 1 21	420.64087	0.00002	19	2 17 - 18 1 17	439.78174	-0.00003
20	2 19 - 21 1 20	421.17243	0.00011	19	2 16 - 18 1 18	439.79767	0.00004
20	2 18 - 21 1 19	421.15091	0.00004	20	2 19 - 19 1 19	440.21967	-0.00003
19	2 17 - 20 1 19	421.65879	0.00000	20	2 18 - 19 1 18	440.20197	-0.00008
18	2 16 - 19 1 18	422.18222	-0.00012	21	2 20 - 20 1 20	440.63962	0.00003
18	2 16 - 19 1 18	422.16449	0.00006	21	2 19 - 20 1 19	440.62003	-0.00002
17	2 16 - 18 1 18	422.66418	0.00006	22	2 20 - 21 1 20	441.03735	0.00005
17	2 15 - 18 1 17	422.66828	-0.00003	22	2 20 - 21 1 20	441.03571	-0.00005
16	2 15 - 17 1 17	423.18402	-0.00001	23	2 22 - 22 1 22	441.47288	0.00006
16	2 14 - 17 1 16	423.16986	-0.00004	23	2 21 - 22 1 21	441.44911	-0.00009
15	2 14 - 16 1 16	423.66189	-0.00002	24	2 23 - 23 1 23	441.88620	0.00006
15	2 13 - 16 1 15	423.66936	0.00001	24	2 22 - 23 1 22	441.86030	-0.00004
14	2 13 - 15 1 15	424.17775	-0.00002	25	2 24 - 24 1 24	442.29731	0.00002
14	2 12 - 15 1 14	424.16670	-0.00002	25	2 23 - 24 1 23	442.26909	-0.00008
13	2 12 - 14 1 14	424.67170	0.00010	25	3 23 - 26 2 25	427.78941	0.00015
13	2 11 - 14 1 13	424.66200	0.00007	24	3 21 - 25 2 23	428.30736	-0.00016
12	2 11 - 13 1 13	425.16340	0.00002	23	3 21 - 24 2 23	428.82234	0.00010
12	2 10 - 13 1 12	425.15310	0.00009				
11	2 10 - 12 1 12	425.63324	0.00012				
11	2 9 - 12 1 11	425.64595	-0.00001				

TABLE I—Continued

J	Ka	Kc	-	J	Ka	Kc	Observed	O-C	J	Ka	Kc	-	J	Ka	Kc	Observed	O-C
22	3	19	-	23	2	21	429.33604	-0.00014	23	3	21	-	22	2	21	450.69414	0.00010
21	3	19	-	22	2	21	429.84707	0.00008	24	3	21	-	23	2	21	451.06828	-0.00016
20	3	17	-	21	2	19	430.35639	-0.00005	25	3	21	-	26	4	23	446.00419	-0.00002
18	3	16	-	19	2	18	431.36877	0.00017	25	3	23	-	24	2	23	451.47561	0.00011
18	3	15	-	19	2	17	431.36877	-0.00008									
17	3	15	-	18	2	17	431.87170	0.00006	25	4	*	-	26	3	*	436.92627	-0.00002
17	3	14	-	18	2	16	431.87170	-0.00015	24	4	*	-	25	3	*	437.44403	-0.00001
16	3	14	-	17	2	16	432.37270	0.00009	23	4	*	-	24	3	*	437.95969	-0.00005
16	3	13	-	17	2	15	432.37270	-0.00007	22	4	*	-	23	3	*	438.47336	0.00000
15	3	13	-	16	2	15	432.87154	0.00005	21	4	*	-	22	3	*	438.98493	0.00001
15	3	12	-	16	2	14	432.87154	-0.00007	20	4	*	-	21	3	*	439.49454	0.00013
14	3	12	-	15	2	14	433.36834	0.00007	19	4	*	-	20	3	*	440.00183	0.00002
14	3	11	-	15	2	13	433.36834	-0.00003	17	4	*	-	18	3	*	441.01032	-0.00004
13	3	11	-	14	2	13	433.86297	0.00001	16	4	*	-	17	3	*	441.51158	0.00001
13	3	10	-	14	2	12	433.86297	-0.00006	15	4	*	-	16	3	*	442.01037	0.00000
12	3	10	-	13	2	12	434.35555	0.00001	14	4	*	-	15	3	*	442.50749	0.00000
12	3	9	-	13	2	11	434.35555	-0.00005	13	4	*	-	14	3	*	443.00227	-0.00005
11	3	9	-	12	2	11	434.84603	0.00000	12	4	*	-	13	3	*	443.49501	-0.00003
11	3	8	-	12	2	10	434.84603	-0.00004	11	4	*	-	12	3	*	443.98567	0.00003
10	3	8	-	11	2	10	435.33437	-0.00003	10	4	*	-	11	3	*	444.47413	0.00000
10	3	7	-	11	2	9	435.33437	-0.00006	8	4	*	-	9	3	*	445.44468	-0.00004
9	3	7	-	10	2	9	435.82082	0.00013	7	4	*	-	8	3	*	445.92686	0.00005
9	3	6	-	10	2	8	435.82082	0.00013	6	4	*	-	7	3	*	446.40678	0.00001
8	3	6	-	9	2	8	436.30478	-0.00004									
8	3	5	-	9	2	7	436.30478	-0.00005	25	4	*	-	25	3	*	449.00036	0.00000
7	3	5	-	8	2	7	436.78687	0.00003	24	4	*	-	24	3	*	449.05433	-0.00011
7	3	4	-	8	2	6	436.78687	0.00002	23	4	*	-	23	3	*	449.10677	-0.00001
6	3	4	-	7	2	6	437.26876	0.00002	22	4	*	-	22	3	*	449.15967	-0.00003
6	3	3	-	7	2	5	437.26876	0.00001	21	4	*	-	21	3	*	449.20446	-0.00003
5	3	3	-	6	2	5	437.74448	-0.00003	20	4	*	-	20	3	*	449.25011	0.00001
5	3	2	-	6	2	4	437.74448	-0.00003	19	4	*	-	19	3	*	449.29351	-0.00003
4	3	2	-	5	2	4	438.22010	-0.00005	18	4	*	-	18	3	*	449.33477	-0.00003
4	3	1	-	5	2	3	438.22010	-0.00005	17	4	*	-	17	3	*	449.37389	-0.00001
									16	4	*	-	16	3	*	449.41082	-0.00001
									15	4	*	-	15	3	*	449.44555	-0.00003
24	3	21	-	24	2	23	439.91828	0.00013	14	4	*	-	14	3	*	449.47814	-0.00003
23	3	21	-	23	2	21	439.97037	-0.00018	13	4	*	-	13	3	*	449.50837	-0.00001
22	3	19	-	22	2	21	440.01984	0.00015	12	4	*	-	12	3	*	449.53680	-0.00002
21	3	19	-	21	2	19	440.06748	-0.00011	11	4	*	-	11	3	*	449.56292	0.00003
20	3	17	-	20	2	19	440.11264	0.00008	10	4	*	-	10	3	*	449.58668	0.00009
19	3	16	-	19	2	18	440.15595	0.00016	9	4	*	-	9	3	*	449.60848	-0.00003
19	3	17	-	19	2	17	440.15595	-0.00009	8	4	*	-	8	3	*	449.62804	-0.00002
18	3	15	-	18	2	17	440.19684	0.00001	7	4	*	-	7	3	*	449.64538	-0.00006
18	3	16	-	18	2	16	440.19684	-0.00019	6	4	*	-	6	3	*	449.66084	-0.00001
17	3	14	-	17	2	16	440.23584	0.00013	5	4	*	-	5	3	*	449.67367	-0.00002
17	3	15	-	17	2	15	440.23584	-0.00003	4	4	*	-	4	3	*	449.68453	-0.00002
16	3	13	-	16	2	15	440.27243	0.00000									
16	3	14	-	16	2	14	440.27243	-0.00013	4	4	*	-	3	3	*	451.94397	-0.00003
15	3	12	-	15	2	14	440.30707	0.00008	5	4	*	-	4	3	*	451.99795	-0.00001
15	3	13	-	15	2	13	440.30707	-0.00002	6	4	*	-	5	3	*	452.44973	-0.00001
14	3	11	-	14	2	13	440.33943	0.00006	7	4	*	-	6	3	*	452.89928	-0.00003
14	3	12	-	14	2	12	440.33943	-0.00002	8	4	*	-	7	3	*	453.34665	-0.00004
13	3	10	-	13	2	12	440.36969	0.00006	9	4	*	-	8	3	*	453.79184	-0.00002
13	3	11	-	13	2	11	440.36969	0.00000	10	4	*	-	9	3	*	454.23477	-0.00004
12	3	9	-	12	2	11	440.39771	0.00000	11	4	*	-	10	3	*	454.67354	-0.00001
12	3	10	-	12	2	10	440.39771	-0.00004	12	4	*	-	11	3	*	455.11405	-0.00002
11	3	8	-	11	2	10	440.42368	0.00006	13	4	*	-	12	3	*	455.55033	-0.00003
11	3	9	-	11	2	9	440.42368	0.00003	14	4	*	-	13	3	*	455.98441	-0.00002
10	3	7	-	10	2	9	440.44736	-0.00002	15	4	*	-	14	3	*	456.41626	-0.00001
10	3	8	-	10	2	8	440.44736	-0.00004	16	4	*	-	15	3	*	456.84586	0.00000
9	3	6	-	9	2	8	440.46897	-0.00001	17	4	*	-	16	3	*	457.27320	-0.00002
9	3	7	-	9	2	7	440.46897	-0.00002	18	4	*	-	17	3	*	457.69834	0.00000
8	3	6	-	8	2	7	440.48847	0.00005	19	4	*	-	18	3	*	458.12116	-0.00004
8	3	7	-	8	2	6	440.48847	0.00004	20	4	*	-	19	3	*	458.54184	0.00002
7	3	4	-	7	2	6	440.48847	0.00017	21	4	*	-	20	3	*	458.96018	0.00001
7	3	5	-	7	2	5	440.50586	0.00016	22	4	*	-	21	3	*	459.37622	-0.00005
6	3	3	-	6	2	5	440.52082	0.00001	23	4	*	-	22	3	*	459.79011	0.00000
6	3	4	-	6	2	4	440.52082	0.00001	24	4	*	-	23	3	*	460.20181	-0.00006
5	3	2	-	5	2	4	440.53382	0.00005	25	4	*	-	24	3	*	460.61091	-0.00005
5	3	3	-	5	2	3	440.53382	0.00005									
4	3	1	-	4	2	3	440.54456	-0.00001									
4	3	2	-	4	2	2	440.54456	-0.00001	25	5	*	-	26	4	*	446.00419	-0.00002
									24	5	*	-	25	4	*	446.32223	-0.00004
3	3	0	-	2	2	0	441.94792	0.00002	23	5	*	-	24	4	*	447.03823	-0.00002
3	3	1	-	2	2	1	441.94792	0.00002	22	5	*	-	23	4	*	447.35221	0.00002
4	3	1	-	3	2	1	442.40413	-0.00001	21	5	*	-	22	4	*	448.06399	-0.00003
4	3	2	-	3	2	2	442.40413	-0.00001	20	5	*	-	21	4	*	448.37384	0.00008
5	3	2	-	4	2	2	442.85820	0.00000	19	5	*	-	20	4	*	449.08141	0.00000
5	3	3	-	4	2	3	442.85820	0.00000	18	5	*	-	19	4	*	449.38688	-0.00007
6	3	3	-	5	2	3	443.31007	-0.00001	17	5	*	-	18	4	*	450.09039	-0.00001
6	3	4	-	5	2	4	443.31007	-0.00001	16	5	*	-	17	4	*	450.39173	-0.00001
7	3	4	-	6	2	4	443.75978	0.00001	15	5	*	-	16	4	*	451.09096	0.00000
7	3	5	-	6	2	5	443.75978	0.00001	14	5	*	-	15	4	*	451.38807	0.00000
8	3	5	-	7	2	5	444.20729	0.00001	13	5	*	-	14	4	*	452.08306	0.00000
8	3	6	-	7	2	6	444.20729	0.00001	12	5	*	-	13	4	*	452.37592	-0.00001
9	3	6	-	8	2	6	444.65237	-0.00002	11	5	*	-	12	4	*	453.06667	0.00001
9	3	7	-	8	2	7	444.65237	-0.00001	10	5	*	-	11	4	*	453.35524	-0.00003
10	3	7	-	9	2	7	445.09572	0.00001	9	5	*	-	10	4	*	454.04169	-0.00004
10	3	8	-	9	2	8	445.09572	0.00003	8	5	*	-	9	4			

TABLE I—Continued

J	Ka	Kc	-	J	Ka	Kc	Observed	O-C	J	Ka	Kc	-	J	Ka	Kc	Observed	O-C
8	5	•	-	8	4	•	458.70899	-0.00004	20	1	19	-	21	2	19	393.29185	0.00000
7	5	•	-	7	4	•	458.72853	-0.00001	20	1	20	-	21	2	20	393.21455	0.00001
6	5	•	-	6	4	•	458.74182	-0.00001	19	1	19	-	20	2	19	393.72441	-0.00007
5	5	•	-	5	4	•	458.75498	0.00003	18	1	17	-	19	2	17	394.72410	-0.00018
9	5	•	-	9	4	•	461.07802	-0.00001	17	1	16	-	18	2	16	394.79391	-0.00006
10	5	•	-	10	4	•	461.53065	-0.00003	16	1	15	-	17	2	15	394.73754	-0.00001
11	5	•	-	11	4	•	461.98011	-0.00001	15	1	14	-	16	2	14	395.28098	-0.00002
12	5	•	-	12	4	•	462.42732	-0.00002	14	1	13	-	15	2	13	395.24102	0.00002
13	5	•	-	13	4	•	462.87230	-0.00003	13	1	12	-	14	2	12	395.78613	-0.00002
14	5	•	-	14	4	•	463.31508	-0.00003	12	1	11	-	13	2	11	396.24090	0.00001
15	5	•	-	15	4	•	463.75580	-0.00005	11	1	10	-	12	2	10	396.77087	-0.00004
16	5	•	-	16	4	•	464.19395	-0.00001	10	1	9	-	11	2	9	397.26046	-0.00001
17	5	•	-	17	4	•	464.63002	-0.00004	9	1	8	-	10	2	8	397.74822	0.00003
18	5	•	-	18	4	•	465.06385	-0.00002	8	1	7	-	9	2	7	397.72399	0.00002
19	5	•	-	19	4	•	465.49544	-0.00002	7	1	6	-	8	2	6	398.21368	-0.00017
20	5	•	-	20	4	•	465.92477	-0.00002	6	1	5	-	7	2	5	398.71798	0.00000
21	5	•	-	21	4	•	466.35183	-0.00004	5	1	4	-	6	2	4	398.70147	0.00000
22	5	•	-	22	4	•	466.77666	-0.00003	4	1	3	-	5	2	3	399.20001	-0.00003
23	5	•	-	23	4	•	467.19927	0.00003	3	1	2	-	4	2	3	399.18688	0.00004
24	5	•	-	24	4	•	467.61950	-0.00003	2	1	1	-	3	2	1	399.68011	-0.00011
25	5	•	-	25	4	•	468.03753	-0.00002	1	1	0	-	2	2	0	399.66998	0.00002
22	0	25	-	23	1	25	400.02878	0.00002	25	1	25	-	25	2	25	402.70746	0.00004
23	0	24	-	24	1	24	400.54657	-0.00004	24	1	24	-	24	2	24	402.82575	0.00001
24	0	23	-	25	1	23	401.06238	-0.00001	23	1	23	-	23	2	23	402.78484	0.00009
25	0	22	-	26	1	22	401.57805	-0.00005	22	1	22	-	22	2	22	402.87397	-0.00005
26	0	21	-	27	1	21	402.08786	0.00013	21	1	21	-	21	2	21	402.81980	0.00001
27	0	20	-	28	1	20	402.59732	0.00003	20	1	20	-	20	2	20	402.92044	0.00007
28	0	19	-	29	1	19	403.10474	-0.00003	19	1	19	-	19	2	19	402.96479	0.00001
29	0	18	-	30	1	18	403.61017	0.00002	18	1	18	-	18	2	18	402.92298	-0.00002
30	0	17	-	31	1	17	404.11347	0.00002	17	1	17	-	17	2	17	403.00733	0.00008
31	0	16	-	32	1	16	404.61469	0.00004	16	1	16	-	16	2	16	403.07120	0.00002
32	0	15	-	33	1	15	405.11374	-0.00001	15	1	15	-	15	2	15	403.04779	-0.00001
33	0	14	-	34	1	14	405.61075	0.00000	14	1	14	-	14	2	14	403.01706	0.00000
34	0	13	-	35	1	13	406.10567	0.00001	13	1	13	-	13	2	13	403.08632	0.00011
35	0	12	-	36	1	12	406.59837	-0.00007	12	1	12	-	12	2	12	403.12508	-0.00002
36	0	11	-	37	1	11	407.08912	0.00001	11	1	11	-	11	2	11	403.16424	-0.00006
37	0	10	-	38	1	10	407.57765	-0.00000	10	1	10	-	10	2	10	403.20340	-0.00004
38	0	9	-	39	1	9	408.06407	-0.00001	9	1	9	-	9	2	9	403.24256	0.00002
39	0	8	-	40	1	8	408.54835	-0.00003	8	1	8	-	8	2	8	403.28172	-0.00003
40	0	7	-	41	1	7	409.03053	-0.00001	7	1	7	-	7	2	7	403.32088	0.00000
41	0	6	-	42	1	6	409.51037	0.00000	6	1	6	-	6	2	6	403.36004	0.00004
42	0	5	-	43	1	5	409.98848	0.00002	5	1	5	-	5	2	5	403.39920	-0.00002
43	0	4	-	44	1	4	411.40925	-0.00001	4	1	4	-	4	2	4	403.43836	0.00001
44	0	3	-	45	1	3	411.87859	0.00003	3	1	3	-	3	2	3	403.47752	0.00009
45	0	2	-	46	1	2	412.13518	0.00000	2	1	2	-	2	2	2	403.51668	-0.00013
46	0	1	-	47	1	1	412.18715	0.00000	1	1	1	-	1	2	1	403.55584	-0.00001
47	0	0	-	48	1	0	412.23698	-0.00005	0	1	0	-	0	2	0	403.59500	0.00004
48	0	0	-	49	1	0	412.28475	-0.00010	0	1	0	-	0	2	0	403.63416	0.00000
49	0	0	-	50	1	0	412.33056	-0.00001	0	1	0	-	0	2	0	403.67332	0.00001
50	0	0	-	51	1	0	412.37417	-0.00005	0	1	0	-	0	2	0	403.71248	0.00001
51	0	0	-	52	1	0	412.41580	0.00001	0	1	0	-	0	2	0	403.75164	0.00000
52	0	0	-	53	1	0	412.45528	0.00000	0	1	0	-	0	2	0	403.79080	-0.00002
53	0	0	-	54	1	0	412.49267	-0.00002	0	1	0	-	0	2	0	403.83000	0.00003
54	0	0	-	55	1	0	412.52801	-0.00001	0	1	0	-	0	2	0	403.86920	0.00000
55	0	0	-	56	1	0	412.56127	0.00000	0	1	0	-	0	2	0	403.90840	0.00004
56	0	0	-	57	1	0	412.59243	-0.00002	0	1	0	-	0	2	0	403.94760	-0.00002
57	0	0	-	58	1	0	412.62154	0.00000	0	1	0	-	0	2	0	403.98680	-0.00003
58	0	0	-	59	1	0	412.64861	0.00003	0	1	0	-	0	2	0	404.02600	0.00000
59	0	0	-	60	1	0	412.67349	-0.00001	0	1	0	-	0	2	0	404.06520	0.00003
60	0	0	-	61	1	0	412.69628	-0.00008	0	1	0	-	0	2	0	404.10440	0.00000
61	0	0	-	62	1	0	412.71713	-0.00001	0	1	0	-	0	2	0	404.14360	0.00004
62	0	0	-	63	1	0	412.73580	-0.00004	0	1	0	-	0	2	0	404.18280	-0.00002
63	0	0	-	64	1	0	412.75250	0.00003	0	1	0	-	0	2	0	404.22200	0.00001
64	0	0	-	65	1	0	412.76717	0.00016	0	1	0	-	0	2	0	404.26120	-0.00004
65	0	0	-	66	1	0	412.77947	-0.00001	0	1	0	-	0	2	0	404.30040	-0.00001
66	0	0	-	67	1	0	412.78988	0.00001	0	1	0	-	0	2	0	404.33960	0.00001
67	0	0	-	68	1	0	412.79818	0.00000	0	1	0	-	0	2	0	404.37880	0.00009
68	0	0	-	69	1	0	412.80447	0.00005	0	1	0	-	0	2	0	404.41800	-0.00013
69	0	0	-	70	1	0	414.19253	0.00002	0	1	0	-	0	2	0	406.19406	-0.00008
70	0	0	-	71	1	0	414.64871	-0.00006	0	1	0	-	0	2	0	406.20188	0.00004
71	0	0	-	72	1	0	415.10284	0.00000	0	1	0	-	0	2	0	406.21000	0.00001
72	0	0	-	73	1	0	415.55468	-0.00004	0	1	0	-	0	2	0	406.21812	0.00000
73	0	0	-	74	1	0	416.45187	-0.00003	0	1	0	-	0	2	0	406.22624	0.00001
74	0	0	-	75	1	0	417.34023	-0.00002	0	1	0	-	0	2	0	406.23436	0.00000
75	0	0	-														

TABLE I—Continued

J	Ka	Kc	-	J	Ka	Kc	Observed	O-C	J	Ka	Kc	-	J	Ka	Kc	Observed	O-C
23	1	23	-	22	2	21	413.50320	-0.00010	15	2	14	-	14	3	12	400.76441	-0.00008
23	1	22	-	22	2	20	413.60491	0.00005	15	2	13	-	14	3	11	400.76441	-0.00002
24	1	24	-	23	2	22	413.91186	-0.00002	16	2	14	-	15	3	12	401.19519	-0.00005
24	1	23	-	23	2	21	414.02233	0.00002	16	2	14	-	15	3	12	401.19519	0.00003
25	1	25	-	24	2	23	414.31805	0.00000	17	2	16	-	16	3	14	401.62372	-0.00010
25	1	24	-	24	2	22	414.43774	0.00000	17	2	15	-	16	3	13	401.62372	0.00000
24	2	23	-	23	3	23	381.80514	-0.00014	18	2	17	-	17	3	15	402.09027	0.00004
22	2	21	-	23	3	21	382.83115	-0.00004	18	2	16	-	17	3	14	402.09027	0.00017
21	2	20	-	22	3	20	383.34104	-0.00011	19	2	18	-	18	3	16	402.47434	-0.00013
21	2	19	-	22	3	19	383.34104	0.00012	19	2	17	-	18	3	15	402.47434	0.00003
20	2	19	-	21	3	19	383.84909	-0.00002	20	2	19	-	19	3	17	402.89853	0.00003
19	2	18	-	20	3	18	383.84909	0.00017	20	2	18	-	19	3	16	402.89853	0.00022
19	2	17	-	20	3	17	384.35492	-0.00015	21	2	20	-	20	3	18	403.31617	-0.00023
18	2	17	-	19	3	17	384.35492	0.00001	21	2	19	-	20	3	17	403.31617	0.00000
18	2	16	-	19	3	16	384.85885	-0.00007	22	2	21	-	21	3	19	403.73407	-0.00002
17	2	16	-	18	3	16	384.85885	0.00006	23	2	22	-	22	3	19	404.14823	-0.00003
17	2	15	-	18	3	15	385.36081	-0.00015	24	2	23	-	23	3	21	404.56284	-0.00008
16	2	15	-	17	3	15	385.36081	-0.00004	25	2	23	-	24	3	21	404.97354	-0.00001
16	2	14	-	17	3	14	385.86087	0.00000	25	3	*	-	26	4	*	371.83873	-0.00002
15	2	14	-	16	3	14	386.35882	-0.00014	24	3	*	-	25	4	*	372.35445	0.00002
14	2	13	-	15	3	13	386.35882	-0.00008	23	3	*	-	24	4	*	372.86809	-0.00003
14	2	12	-	15	3	12	386.85439	-0.00003	22	3	*	-	23	4	*	373.37984	0.00001
13	2	12	-	14	3	12	386.85439	0.00001	21	3	*	-	22	4	*	373.88957	0.00001
13	2	11	-	14	3	11	387.34842	-0.00003	20	3	*	-	21	4	*	374.39732	0.00003
12	2	11	-	13	3	11	387.34842	0.00000	18	3	*	-	19	4	*	375.40678	0.00003
12	2	10	-	13	3	10	387.84024	-0.00002	17	3	*	-	18	4	*	375.90849	0.00001
11	2	10	-	12	3	10	387.84024	0.00002	16	3	*	-	17	4	*	376.40819	0.00000
11	2	9	-	12	3	9	388.32990	-0.00009	15	3	*	-	16	4	*	376.90591	0.00001
10	2	9	-	11	3	9	388.32990	-0.00007	14	3	*	-	15	4	*	377.40181	0.00004
10	2	8	-	11	3	8	388.81773	0.00003	13	3	*	-	14	4	*	377.89520	-0.00002
9	2	8	-	10	3	8	388.81773	0.00005	12	3	*	-	13	4	*	378.38663	-0.00001
9	2	7	-	10	3	7	389.30330	-0.00004	11	3	*	-	12	4	*	378.87648	0.00003
8	2	7	-	9	3	7	389.30330	-0.00004	10	3	*	-	11	4	*	379.36401	0.00003
8	2	6	-	9	3	6	389.78694	0.00001	9	3	*	-	10	4	*	379.84945	-0.00004
7	2	6	-	8	3	6	389.78694	0.00001	8	3	*	-	9	4	*	380.33297	0.00003
7	2	5	-	8	3	5	390.26848	0.00002	7	3	*	-	8	4	*	380.81439	0.00004
6	2	5	-	7	3	5	390.26848	0.00002	6	3	*	-	7	4	*	381.29370	0.00000
6	2	4	-	7	3	4	390.74791	-0.00001	5	3	*	-	6	4	*	381.77096	-0.00003
5	2	4	-	6	3	4	390.74791	-0.00001	4	3	*	-	5	4	*	382.24623	0.00003
5	2	3	-	6	3	3	391.22529	-0.00002	3	3	*	-	4	4	*	382.71936	-0.00002
4	2	3	-	5	3	3	391.22529	-0.00002	25	3	*	-	25	4	*	383.91178	0.00000
4	2	2	-	5	3	2	391.70058	-0.00005	24	3	*	-	24	4	*	383.96399	-0.00004
3	2	2	-	4	3	2	392.17387	0.00001	23	3	*	-	23	4	*	384.01416	-0.00003
3	2	1	-	4	3	1	392.17387	0.00001	22	3	*	-	22	4	*	384.06226	0.00000
2	2	1	-	3	3	1	392.64506	0.00004	21	3	*	-	21	4	*	384.10823	0.00000
2	2	0	-	3	3	0	392.64506	0.00004	20	3	*	-	20	4	*	384.15216	0.00001
25	2	23	-	23	3	23	393.36305	0.00010	19	3	*	-	19	4	*	384.19394	-0.00001
24	2	23	-	24	3	21	393.41383	-0.00003	18	3	*	-	18	4	*	384.23371	0.00004
23	2	21	-	23	3	21	393.46396	0.00005	17	3	*	-	17	4	*	384.27134	0.00004
22	2	21	-	22	3	19	393.91448	-0.00005	16	3	*	-	16	4	*	384.30689	0.00005
21	2	20	-	21	3	18	393.96056	-0.00015	15	3	*	-	15	4	*	384.34028	-0.00002
21	2	19	-	21	3	17	393.96056	0.00009	14	3	*	-	14	4	*	384.37185	-0.00001
20	2	19	-	20	3	17	393.96056	-0.00008	13	3	*	-	13	4	*	384.40088	-0.00005
20	2	18	-	20	3	16	393.96056	0.00012	12	3	*	-	12	4	*	384.42810	-0.00001
19	2	18	-	19	3	16	393.96056	-0.00002	11	3	*	-	11	4	*	384.45322	0.00002
19	2	17	-	19	3	15	393.96056	0.00014	10	3	*	-	10	4	*	384.47833	0.00003
18	2	17	-	18	3	15	393.96056	-0.00003	9	3	*	-	9	4	*	384.49710	-0.00001
18	2	16	-	18	3	14	393.96056	0.00010	8	3	*	-	8	4	*	384.51590	-0.00003
17	2	16	-	17	3	14	393.96056	-0.00008	7	3	*	-	7	4	*	384.53272	0.00006
16	2	15	-	16	3	13	393.96056	0.00002	6	3	*	-	6	4	*	384.54725	-0.00005
16	2	14	-	16	3	12	393.96056	-0.00001	5	3	*	-	5	4	*	384.55973	-0.00011
15	2	13	-	15	3	12	393.96056	0.00007	4	3	*	-	4	4	*	384.57032	0.00002
15	2	12	-	15	3	11	393.96056	0.00004	7	3	*	-	6	4	*	387.78635	0.00010
14	2	12	-	14	3	11	393.96056	-0.00001	8	3	*	-	7	4	*	388.23427	0.00003
14	2	11	-	14	3	10	393.96056	0.00001	9	3	*	-	8	4	*	388.68001	-0.00009
13	2	11	-	13	3	10	393.96056	-0.00003	10	3	*	-	9	4	*	389.12373	-0.00010
13	2	10	-	13	3	9	393.96056	0.00004	11	3	*	-	10	4	*	389.56547	0.00005
12	2	10	-	12	3	8	393.96056	-0.00003	12	3	*	-	11	4	*	389.90490	0.00002
12	2	9	-	12	3	7	393.96056	0.00001	13	3	*	-	12	4	*	390.44212	-0.00007
11	2	9	-	11	3	6	393.96056	-0.00003	14	3	*	-	13	4	*	390.87739	0.00003
11	2	8	-	11	3	5	393.96056	0.00001	15	3	*	-	14	4	*	391.31055	-0.00003
10	2	8	-	10	3	4	393.96056	-0.00001	16	3	*	-	15	4	*	391.74132	0.00008
9	2	8	-	9	3	3	393.96056	0.00001	17	3	*	-	16	4	*	392.16991	-0.00004
9	2	7	-	9	3	2	393.96056	-0.00001	18	3	*	-	17	4	*	392.59648	-0.00001
8	2	7	-	8	3	1	393.96056	0.00001	19	3	*	-	18	4	*	393.02083	-0.00003
8	2	6	-	8	3	0	393.96056	-0.00002	20	3	*	-	19	4	*	393.44307	0.00000
7	2	6	-	7	3	0	393.96056	0.00002	21	3	*	-	20	4	*	393.86314	0.00005
7	2	5	-	7	3	0	393.96056	0.00003	22	3	*	-	21	4	*	394.28093	-0.00001
6	2	5	-	6	3	0	394.00181	0.00002	23	3	*	-	22	4	*	394.69683	0.00021
6	2	4	-	6	3	0	394.00181	0.00002	24	3	*	-	23	4	*	395.11004	-0.00006
5	2	4	-	5	3	0	394.01445	0.00005	25	3	*	-	24	4	*	395.52148	0.00009
5	2	3	-	5	3	0	394.01445	0.00005	25	4	*	-	26	5	*	362.34313	0.00002
4	2	3	-	4	3	0	394.02499	0.00007	24	4	*	-	25	5	*	362.85852	0.00003
4	2	2	-	4	3	0	394.02499	0.00007	23	4	*	-	24	5	*	363.37194	-0.00002
3	2	2	-	3	3	0	394.03323	-0.00009	22	4	*	-	23	5	*	363.88333	0.00004
3	2	1	-	3	3	0	394.03323	-0.00009	21	4	*	-	22	5	*	364.39285	0.00004
7	2	6															

TABLE I—Continued

J	Ka	Kc	-	J	Ka	Kc	Observed	O-C	J	Ka	Kc	-	J	Ka	Kc	Observed	O-C
23	4			23	5		374.41484	0.00003	23	1	25		23	0	23	394.38403	-0.00006
24	4			24	5		374.46684	0.00003	24	1	24		24	0	24	394.44441	-0.00006
23	4			23	5		374.51674	0.00000	23	1	23		23	0	23	394.50228	-0.00018
22	4			22	5		374.56459	0.00000	22	1	22		22	0	22	394.55782	-0.00018
21	4			21	5		374.61034	-0.00003	21	1	21		21	0	21	394.61096	-0.00015
20	4			20	5		374.65413	0.00007	20	1	20		20	0	20	394.66177	-0.00015
19	4			19	5		374.69569	0.00001	19	1	19		19	0	19	394.70992	-0.00019
18	4			18	5		374.73524	0.00003	18	1	18		18	0	18	394.75588	-0.00010
17	4			17	5		374.77266	-0.00001	17	1	17		17	0	17	394.79923	-0.00019
16	4			16	5		374.80809	0.00004	16	1	16		16	0	16	394.84030	-0.00018
15	4			15	5		374.84135	0.00000	14	1	14		14	0	14	394.87512	-0.00019
14	4			14	5		374.87251	-0.00005	13	1	13		13	0	13	394.94891	-0.00019
12	4			12	5		374.92879	0.00004	11	1	11		11	0	11	395.00930	-0.00014
11	4			11	5		374.95372	-0.00001	9	1	9		9	0	9	395.05990	-0.00022
10	4			10	5		374.97845	-0.00001	7	1	7		7	0	7	395.10098	-0.00017
9	4			9	5		374.99745	0.00001	8	1	7		7	0	7	398.80917	-0.00013
8	4			8	5		375.01625	0.00008	10	1	9		9	0	9	399.70205	-0.00009
7	4			7	5		375.03288	0.00006	11	1	10		10	0	10	400.14587	-0.00008
6	4			6	5		375.04741	0.00002	12	1	11		11	0	11	400.58783	-0.00018
5	4			5	5		375.05989	0.00001	14	1	13		13	0	13	401.46668	-0.00013
9	4			9	5		379.17980	-0.00016	16	1	15		15	0	15	402.33844	-0.00014
11	4			11	5		380.06542	0.00003	17	1	16		16	0	16	402.77167	-0.00015
12	4			12	5		380.50503	0.00012	18	1	17		17	0	17	403.20316	-0.00011
13	4			13	5		380.94223	-0.00005	19	1	18		18	0	18	403.63294	-0.00001
14	4			14	5		381.37771	-0.00014	20	1	19		19	0	19	404.06070	-0.00015
15	4			15	5		381.81089	0.00005	22	1	21		21	0	21	404.91104	-0.00023
16	4			16	5		382.24186	0.00003	25	2	24		24	1	24	391.75845	0.00006
17	4			17	5		382.67041	-0.00004	25	2	23		23	1	23	391.62807	0.00010
19	4			19	5		383.52161	-0.00001	24	2	23		23	1	23	392.28497	0.00018
20	4			20	5		383.94391	-0.00006	24	2	22		22	1	22	392.77156	0.00014
21	4			21	5		384.36405	-0.00010	23	2	22		22	1	22	392.66178	0.00012
22	4			22	5		384.78229	0.00013	23	2	21		21	1	21	393.27644	0.00017
23	4			23	5		385.19797	-0.00002	22	2	21		21	1	21	393.17548	0.00020
23	4			23	5		386.02317	0.00004	19	2	17		17	1	17	394.70327	0.00004
25	5			25	6		352.80439	0.00010	18	2	17		17	1	17	395.27798	0.00019
24	5			24	6		353.31958	-0.00002	18	2	16		16	1	16	395.20837	0.00014
23	5			23	6		353.83289	0.00014	17	2	16		16	1	16	395.77368	0.00000
22	5			22	6		354.34377	0.00004	17	2	15		15	1	15	395.71127	0.00020
21	5			21	6		354.85298	0.00003	16	2	15		15	1	15	396.28797	0.00022
20	5			20	6		355.36018	0.00001	16	2	14		14	1	14	396.21188	0.00013
19	5			19	6		355.86543	0.00001	15	2	13		13	1	13	396.71033	0.00014
18	5			18	6		356.36873	0.00004	14	2	13		13	1	13	397.25087	0.00022
17	5			17	6		356.87004	0.00007	12	2	11		11	1	11	398.22607	0.00021
16	5			16	6		357.36928	0.00002	12	2	10		10	1	10	398.19285	0.00012
15	5			15	6		357.86650	-0.00003	10	2	8		8	1	8	399.18683	0.00014
14	5			14	6		358.36189	0.00003	8	2	7		7	1	7	400.13478	0.00014
13	5			13	6		358.85513	0.00003	23	2	23		23	1	23	403.77182	0.00013
12	5			12	6		359.34646	0.00006	24	2	22		22	1	22	403.81903	0.00017
11	5			11	6		359.83589	0.00004	22	2	21		21	1	21	403.81491	0.00011
10	5			10	6		360.32283	0.00004	21	2	19		19	1	19	403.84931	0.00020
9	5			9	6		360.80810	0.00000	21	2	20		20	1	20	403.86438	-0.00003
8	5			8	6		361.29128	0.00000	20	2	18		18	1	18	403.98877	0.00000
7	5			7	6		361.77249	0.00007	20	2	17		17	1	17	403.91184	0.00007
6	5			6	6		362.25155	0.00002	17	2	15		15	1	15	404.09659	0.00016
5	5			5	6		362.72863	0.00004	17	2	16		16	1	16	404.04058	0.00021
23	5			23	6		364.87442	0.00006	15	2	13		13	1	13	404.15897	0.00018
24	5			24	6		364.92613	-0.00001	14	2	12		12	1	12	404.18723	0.00009
23	5			23	6		364.97590	0.00002	13	2	12		12	1	12	404.18033	0.00008
22	5			22	6		365.02359	0.00006	12	2	10		10	1	10	404.23835	0.00018
21	5			21	6		365.06916	0.00004	12	2	11		11	1	11	404.20978	0.00019
20	5			20	6		365.11281	-0.00002	10	2	9		9	1	9	404.26136	-0.00014
19	5			19	6		365.15412	0.00003	4	2	3		3	1	3	406.21730	0.00016
18	5			18	6		365.19346	0.00001	6	2	5		5	1	5	407.12147	0.00003
17	5			17	6		365.23081	0.00006	8	2	4		4	1	4	407.11589	-0.00006
16	5			16	6		365.26600	0.00002	8	2	7		7	1	7	408.01829	0.00022
15	5			15	6		365.29914	0.00000	8	2	6		6	1	6	408.00798	0.00016
14	5			14	6		365.33020	-0.00003	11	2	9		9	1	9	409.32847	0.00004
13	5			13	6		365.35929	0.00003	12	2	11		11	1	11	409.78837	0.00016
12	5			12	6		365.38624	0.00003	12	2	10		10	1	10	409.76399	-0.00003
11	5			11	6		365.41106	0.00002	13	2	12		12	1	12	410.22890	0.00010
10	5			10	6		365.43384	-0.00002	13	2	10		10	1	10	411.52739	0.00010
9	5			9	6		365.45459	0.00001	16	2	15		15	1	15	412.81118	0.00009
8	5			8	6		365.47324	0.00000	19	2	18		18	1	18	413.23528	0.00019
7	5			7	6		365.48996	-0.00018	20	2	18		18	1	18	413.16570	0.00015
6	5			6	6		365.50428	-0.00003	20	2	19		19	1	19	413.63710	-0.00002
10	5			10	6		370.08039	0.00006	22	2	21		21	1	21	414.07720	0.00003
11	5			11	6		370.52195	-0.00007	23	2	22		22	1	22	414.49538	0.00013
12	5			12	6		370.96185	0.00006	24	2	23		23	1	23	414.91149	0.00014
13	5			13	6		371.39906	0.00003	24	2	22		22	1	22	414.81031	0.00013
14	5			14	6		371.83421	-0.00013	25	2	24		24	1	24	415.32340	-0.00006
15	5			15	6		372.26753	0.00002	25	2	23		23	1	23	415.21590	0.00018
16	5			16	6		372.69859	0.00004	24	3	22		22	2	22	401.37302	0.00017
17	5			17	6		373.12761	0.00015	23	3	21		21	2	21	401.88456	-0.00001
18	5			18	6		373.55412	-0.00009	22	3	20		20	2	20	402.39441	0.00011
19	5			19	6		373.97884	0.00002	20	3	18		18	2	18	403.40766	-0.00012
20	5			20	6		374.40132	0.00003	19	3	16		16	2	16	403.91184	0.00013
21	5			21	6		374.82167	0.00010	18	3	16		16	2	16	404.41330	0.00006
22	5			22	6		375.23964	-0.0000									

TABLE I—Continued

J	Ka	Kc	-	J	Ka	Kc	Observed	O-C	J	Ka	Kc	-	J	Ka	Kc	Observed	O-C
22	3	19	-	22	2	21	413.02920	-0.00017	26	5	*	-	27	4	*	418.33556	-0.00013
21	3	18	-	21	2	20	413.07346	0.00004	25	5	*	-	26	4	*	419.05262	0.00003
21	3	19	-	21	2	19	413.07346	-0.00020	24	5	*	-	25	4	*	419.36742	-0.00005
20	3	17	-	20	2	18	413.11932	-0.00006	23	5	*	-	24	4	*	420.08031	0.00020
19	3	16	-	19	2	18	413.18116	-0.00009	22	5	*	-	23	4	*	420.39110	-0.00001
18	3	15	-	18	2	17	413.20089	-0.00013	21	5	*	-	22	4	*	421.10001	0.00014
17	3	14	-	17	2	16	413.23861	-0.00008	20	5	*	-	21	4	*	421.60660	0.00002
16	3	13	-	16	2	15	413.27413	-0.00015	19	5	*	-	20	4	*	423.11429	-0.00009
15	3	12	-	15	2	14	413.30770	-0.00007	18	5	*	-	19	4	*	423.61280	-0.00006
15	3	13	-	15	2	13	413.30770	-0.00013	17	5	*	-	18	4	*	425.09581	-0.00006
13	3	10	-	13	2	12	413.36834	-0.00013	16	5	*	-	17	4	*	426.07411	-0.00002
13	3	11	-	13	2	11	413.36834	-0.00016	15	5	*	-	16	4	*	426.36010	-0.00003
12	3	9	-	12	2	11	413.39562	-0.00006	14	5	*	-	15	4	*	431.12383	0.00005
12	3	10	-	12	2	10	413.39562	-0.00008	24	5	*	-	24	4	*	431.22442	-0.00008
11	3	8	-	11	2	10	413.42068	-0.00011	22	5	*	-	22	4	*	431.31661	-0.00005
11	3	9	-	11	2	9	413.42068	-0.00013	20	5	*	-	20	4	*	431.40014	-0.00011
9	3	*	-	10	2	*	413.44373	-0.00007	18	5	*	-	18	4	*	431.43871	-0.00012
8	3	*	-	9	2	*	413.46468	-0.00007	17	5	*	-	17	4	*	431.47321	-0.00006
7	3	*	-	8	2	*	413.48331	-0.00009	16	5	*	-	16	4	*	431.50951	-0.00005
6	3	*	-	7	2	*	413.50024	0.00000	15	5	*	-	15	4	*	431.54171	0.00000
6	3	*	-	6	2	*	413.51498	-0.00014	14	5	*	-	14	4	*	431.57174	0.00002
5	3	*	-	5	2	*	413.52740	-0.00014	13	5	*	-	13	4	*	431.59963	0.00004
3	3	*	-	2	2	*	414.93453	-0.00014	12	5	*	-	12	4	*	431.62333	0.00002
4	3	*	-	3	2	*	415.38909	0.00005	11	5	*	-	11	4	*	431.64892	0.00005
5	3	*	-	4	2	*	415.84115	-0.00016	10	5	*	-	10	4	*	431.67031	-0.00002
6	3	*	-	5	2	*	416.29144	-0.00002	9	5	*	-	9	4	*	431.68972	0.00010
7	3	*	-	6	2	*	416.73937	-0.00012	8	5	*	-	8	4	*	431.70681	0.00004
8	3	*	-	7	2	*	417.18536	-0.00003	7	5	*	-	7	4	*	431.73452	-0.00012
9	3	*	-	8	2	*	417.62906	-0.00012	5	5	*	-	5	4	*	434.04612	0.00007
10	3	*	-	9	2	*	418.07073	-0.00009	6	5	*	-	6	4	*	434.49763	0.00000
11	3	8	-	10	2	8	418.51026	-0.00010	7	5	*	-	7	4	*	434.94543	0.00000
11	3	9	-	10	2	9	418.51026	-0.00008	8	5	*	-	8	4	*	435.39092	0.00008
12	3	10	-	11	2	10	418.94782	0.00011	9	5	*	-	9	4	*	435.83405	-0.00007
12	3	9	-	11	2	9	418.94782	0.00009	10	5	*	-	10	4	*	436.27315	-0.00004
13	3	11	-	12	2	11	419.38279	-0.00015	11	5	*	-	11	4	*	436.71402	-0.00008
13	3	10	-	12	2	10	419.38279	-0.00018	12	5	*	-	12	4	*	437.15073	0.00005
15	3	13	-	14	2	13	420.24686	-0.00008	13	5	*	-	13	4	*	437.58542	-0.00002
15	3	12	-	14	2	12	420.24686	-0.00013	14	5	*	-	14	4	*	438.01755	-0.00002
16	3	14	-	15	2	14	420.67563	-0.00008	15	5	*	-	15	4	*	438.44763	-0.00003
16	3	13	-	15	2	13	420.67563	-0.00014	16	5	*	-	16	4	*	438.87364	0.00009
17	3	15	-	16	2	15	421.10224	-0.00007	17	5	*	-	17	4	*	439.30115	-0.00007
17	3	14	-	16	2	14	421.10224	-0.00015	18	5	*	-	18	4	*	439.72473	0.00005
18	3	16	-	17	2	16	421.52658	-0.00017	19	5	*	-	19	4	*	440.14585	-0.00007
19	3	17	-	18	2	17	421.94886	-0.00016	20	5	*	-	20	4	*	440.56482	-0.00012
20	3	18	-	19	2	18	422.36908	-0.00003	21	5	*	-	21	4	*	440.98172	-0.00001
20	3	17	-	19	2	17	422.36908	-0.00018	22	5	*	-	22	4	*	441.39619	-0.00010
21	3	19	-	20	2	19	422.78693	-0.00009	23	5	*	-	23	4	*	441.80855	-0.00006
23	3	21	-	22	2	21	423.61619	-0.00011	24	5	*	-	24	4	*	442.21873	0.00004
24	3	21	-	23	2	21	424.02785	-0.00012	25	5	*	-	25	4	*	442.62654	0.00002
25	3	23	-	24	2	23	424.43660	-0.00019	25	5	*	-	25	4	*	373.15892	-0.00012
25	4	*	-	26	3	*	409.98073	0.00006	23	0	25	-	24	1	23	374.18194	0.00003
23	4	*	-	24	3	*	411.00709	0.00002	21	0	21	-	22	1	21	375.21632	0.00014
22	4	*	-	23	3	*	411.51720	-0.00006	20	0	20	-	21	1	20	375.72493	-0.00016
20	4	*	-	21	3	*	412.53149	-0.00012	19	0	19	-	20	1	19	376.23173	-0.00012
19	4	*	-	20	3	*	413.03588	0.00014	18	0	18	-	19	1	18	376.73654	0.00007
18	4	*	-	19	3	*	413.53780	-0.00004	17	0	17	-	18	1	17	377.23895	0.00004
17	4	*	-	18	3	*	414.03790	-0.00002	16	0	16	-	17	1	16	377.73901	-0.00017
16	4	*	-	17	3	*	414.53579	-0.00017	15	0	15	-	16	1	15	378.23742	0.00012
15	4	*	-	16	3	*	415.03201	0.00006	13	0	13	-	14	1	13	379.22714	0.00013
14	4	*	-	15	3	*	415.52599	0.00009	12	0	12	-	13	1	12	379.71674	0.00014
12	4	*	-	13	3	*	416.90781	0.00016	11	0	11	-	12	1	11	380.20812	0.00010
11	4	*	-	12	3	*	416.99538	-0.00006	9	0	9	-	10	1	9	381.18032	0.00003
9	4	*	-	10	3	*	417.96469	-0.00014	8	0	8	-	9	1	8	381.66332	0.00017
25	4	*	-	25	3	*	421.99936	-0.00001	7	0	7	-	8	1	7	382.14395	0.00014
22	4	*	-	22	3	*	422.15155	-0.00007	3	0	3	-	4	1	3	384.04456	0.00010
21	4	*	-	21	3	*	422.19821	0.00007	25	0	25	-	25	1	25	385.30232	-0.00024
20	4	*	-	20	3	*	422.24256	0.00001	24	0	24	-	24	1	24	385.34946	-0.00008
19	4	*	-	19	3	*	422.28482	-0.00003	23	0	23	-	23	1	23	385.39454	0.00011
18	4	*	-	18	3	*	422.32508	0.00005	22	0	22	-	22	1	22	385.43753	0.00010
17	4	*	-	17	3	*	422.36304	-0.00006	21	0	21	-	21	1	21	385.47853	-0.00001
16	4	*	-	16	3	*	422.39902	-0.00004	20	0	20	-	20	1	20	385.51780	-0.00001
15	4	*	-	15	3	*	422.43286	0.00006	19	0	19	-	19	1	19	385.55524	0.00007
14	4	*	-	14	3	*	422.46469	0.00000	18	0	18	-	18	1	18	385.59076	0.00010
13	4	*	-	13	3	*	422.49424	0.00005	17	0	17	-	17	1	17	385.62439	0.00012
12	4	*	-	12	3	*	422.52179	0.00005	16	0	16	-	16	1	16	385.65607	0.00007
11	4	*	-	11	3	*	422.54715	0.00003	15	0	15	-	15	1	15	385.68595	0.00006
10	4	*	-	10	3	*	422.57047	0.00008	14	0	14	-	14	1	14	385.71393	0.00006
9	4	*	-	9	3	*	422.59153	-0.00001	13	0	13	-	13	1	13	385.74012	0.00012
8	4	*	-	8	3	*	422.61054	-0.00004	12	0	12	-	12	1	12	385.76432	0.00007
7	4	*	-	7	3	*	422.62769	0.00019	11	0	11	-	11	1	11	385.78669	0.00006
6	4	*	-	6	3	*	422.64225	-0.00006	9	0	9	-	9	1	9	385.82378	-0.00002
5	4	*	-	5	3	*	422.65300	0.00000	8	0	8	-	8	1	8	385.84256	-0.00002
4	4	*	-	4	3	*	424.51658	0.00007	7	0	7	-	7	1	7	385.85736	-0.00013
6	4	*	-	5	3	*	424.96838	-0.00005	6	0	6	-	6	1	6	385.87067	0.00013
6	4	*	-	5	3	*	425.41871	0.00009	5	0	5	-	5	1	5	385.88172	-0.00001
7	4	*	-	6	3	*	425.86647	0.00001	5	0	5	-	4	1	5	388.19093	-0.00006
9	4	*	-	8	3	*	426.75369	-0.00002	7	0	7	-	6	1	7	389.08768	-0.00015
10	4																

TABLE I—Continued

J	Ka	Kc	-	J	Ka	Kc	Observed	O-C	J	Ka	Kc	-	J	Ka	Kc	Observed	O-C
17	1	16	-	18	2	16	368.02723	-0.00003	24	3	•	-	24	4	•	357.29201	-0.00021
16	1	15	-	17	2	15	368.51783	-0.00013	23	3	•	-	23	4	•	357.34058	-0.00004
15	1	14	-	16	2	14	369.00690	-0.00015	21	3	•	-	21	4	•	357.43150	-0.00015
14	1	13	-	15	2	13	369.49451	-0.00002	20	3	•	-	20	4	•	357.47389	-0.00019
13	1	13	-	14	2	13	369.91572	-0.00021	19	3	•	-	19	4	•	357.51448	-0.00002
13	1	12	-	14	2	12	369.98041	0.00002	18	3	•	-	18	4	•	357.55280	0.00000
12	1	11	-	13	2	11	370.46460	-0.00004	18	3	•	-	16	4	•	357.62370	0.00006
11	1	11	-	12	2	11	370.90044	-0.00010	15	3	•	-	15	4	•	357.65560	-0.00008
10	1	10	-	11	2	10	371.36933	0.00001	13	3	•	-	13	4	•	357.71449	-0.00011
8	1	7	-	9	2	7	372.36524	-0.00009	12	3	•	-	12	4	•	357.74071	-0.00017
6	1	5	-	7	2	5	373.33583	0.00000	10	3	•	-	10	4	•	357.78740	0.00002
									9	3	•	-	9	4	•	357.80760	0.00000
25	1	25	-	25	2	25	375.83299	-0.00004	8	3	•	-	8	4	•	357.82561	-0.00018
23	1	23	-	23	2	21	375.95027	-0.00004	7	3	•	-	7	4	•	357.84178	-0.00019
21	1	21	-	21	2	19	376.05761	-0.00014									
20	1	19	-	20	2	19	376.25679	-0.00014	21	3	•	-	20	4	•	367.14179	0.00006
20	1	20	-	20	2	18	376.10802	-0.00021	22	3	•	-	21	4	•	367.35884	-0.00014
14	1	13	-	14	2	13	376.43346	-0.00018	25	3	•	-	24	4	•	368.79798	-0.00003
13	1	13	-	13	2	11	376.39289	-0.00014									
10	1	10	-	10	2	8	376.47877	-0.00010	25	4	•	-	26	5	•	339.81767	-0.00003
5	1	4	-	4	2	2	378.89874	-0.00012	23	4	•	-	24	5	•	338.83928	0.00006
10	1	9	-	9	2	7	381.14474	-0.00006	22	4	•	-	23	5	•	337.34715	0.00003
11	1	10	-	10	2	8	381.38883	0.00000	21	4	•	-	22	5	•	337.85317	0.00008
13	1	13	-	12	2	11	382.40722	-0.00003	20	4	•	-	21	5	•	338.35725	0.00011
14	1	13	-	13	2	11	382.91056	0.00002	19	4	•	-	20	5	•	338.85918	-0.00009
15	1	13	-	14	2	13	383.26246	-0.00014	18	4	•	-	19	5	•	339.35936	-0.00010
15	1	14	-	14	2	12	383.34763	0.00000	17	4	•	-	18	5	•	339.85765	-0.00007
17	1	17	-	16	2	15	384.10825	0.00016	16	4	•	-	17	5	•	340.35405	0.00002
18	1	18	-	17	2	16	384.52704	-0.00009	15	4	•	-	16	5	•	340.84837	-0.00004
18	1	17	-	17	2	15	384.64853	0.00012	14	4	•	-	15	5	•	341.34096	0.00013
19	1	19	-	18	2	17	384.94355	-0.00014	13	4	•	-	14	5	•	341.83126	-0.00004
19	1	18	-	18	2	16	385.07843	-0.00007	12	4	•	-	13	5	•	342.31988	-0.00007
21	1	21	-	20	2	19	385.76935	-0.00001	11	4	•	-	12	5	•	342.80827	-0.00009
25	1	25	-	24	2	23	387.39075	0.00005	10	4	•	-	11	5	•	343.29089	-0.00005
									9	4	•	-	10	5	•	343.77368	0.00014
									6	4	•	-	7	5	•	345.20956	0.00007
25	2	24	-	26	3	24	354.99538	0.00001	25	4	•	-	25	5	•	347.83390	-0.00001
25	2	25	-	26	3	25	354.99538	-0.00016	24	4	•	-	24	5	•	347.88450	0.00012
21	2	20	-	22	3	20	356.63188	0.00014	23	4	•	-	23	5	•	347.93290	0.00006
21	2	19	-	22	3	19	356.63188	0.00006	22	4	•	-	22	5	•	347.97928	0.00001
19	2	18	-	20	3	18	357.63860	0.00022	21	4	•	-	21	5	•	348.02372	0.00003
19	2	17	-	20	3	17	357.63860	0.00016	20	4	•	-	20	5	•	348.06596	-0.00011
17	2	16	-	18	3	16	358.63750	0.00018	19	4	•	-	19	5	•	348.10839	-0.00009
17	2	15	-	18	3	15	358.63750	0.00018	18	4	•	-	18	5	•	348.14478	-0.00006
16	2	15	-	17	3	15	359.13399	0.00018	17	4	•	-	17	5	•	348.18128	0.00009
16	2	14	-	17	3	14	359.13399	0.00015	16	4	•	-	16	5	•	348.21567	0.00015
13	2	12	-	14	3	12	360.61181	0.00012	15	4	•	-	15	5	•	348.24780	0.00007
13	2	11	-	14	3	11	360.61181	0.00011	14	4	•	-	14	5	•	348.27808	-0.00005
12	2	•	-	13	3	•	361.10031	-0.00008	13	4	•	-	13	5	•	348.30819	-0.00021
11	2	•	-	12	3	•	361.58731	0.00019	12	4	•	-	12	5	•	348.33280	0.00015
									11	4	•	-	11	5	•	348.35709	0.00020
25	2	25	-	25	3	23	366.61429	0.00006	9	4	•	-	9	5	•	348.39948	0.00018
24	2	25	-	24	3	22	366.66486	0.00003	8	4	•	-	8	5	•	348.41749	0.00001
24	2	23	-	24	3	21	366.66486	0.00016									
23	2	21	-	23	3	21	366.71360	0.00018									
22	2	20	-	22	3	20	366.76008	0.00010	18	4	•	-	17	5	•	356.46819	-0.00012
22	2	21	-	22	3	19	366.76008	0.00020	21	4	•	-	20	5	•	357.73259	-0.00004
21	2	19	-	21	3	19	366.80472	0.00019	22	4	•	-	21	5	•	358.14970	-0.00016
20	2	18	-	20	3	18	366.84720	0.00015	23	4	•	-	22	5	•	358.56511	0.00013
20	2	19	-	20	3	17	366.84720	0.00021	24	4	•	-	23	5	•	358.97780	-0.00018
19	2	17	-	19	3	17	366.88764	0.00008	25	4	•	-	24	5	•	359.38891	0.00004
19	2	18	-	19	3	16	366.88764	0.00013									
18	2	18	-	18	3	16	366.92615	0.00010									
18	2	17	-	18	3	15	366.92615	0.00015									
17	2	15	-	17	3	15	366.96256	0.00005	24	1	23	-	25	0	23	383.08576	-0.00001
17	2	16	-	17	3	14	366.96256	0.00009	22	1	21	-	23	0	23	384.08912	0.00011
15	2	15	-	15	3	15	367.02942	0.00005	21	1	20	-	22	0	22	384.38829	0.00007
15	2	14	-	15	3	12	367.02942	0.00007	20	1	19	-	21	0	21	385.08585	0.00003
12	2	10	-	12	3	10	367.11483	0.00015	16	1	15	-	17	0	17	387.08009	0.00006
12	2	11	-	12	3	9	367.11483	0.00018	14	1	13	-	15	0	15	388.03794	0.00017
9	2	•	-	9	3	•	367.18143	0.00006	10	1	9	-	11	0	11	389.97240	0.00007
4	2	•	-	3	3	•	369.10312	-0.00013	25	1	25	-	25	0	25	394.37100	0.00001
5	2	•	-	4	3	•	369.55573	-0.00008	24	1	24	-	24	0	24	394.43142	0.00009
6	2	•	-	5	3	•	370.00641	0.00009	23	1	23	-	23	0	23	394.49443	0.00017
7	2	•	-	6	3	•	370.45481	0.00003	22	1	22	-	22	0	22	394.54501	0.00023
9	2	•	-	8	3	•	371.34372	0.00018	21	1	21	-	21	0	21	394.59811	0.00021
10	2	•	-	9	3	•	371.78904	0.00023	20	1	20	-	20	0	20	394.64877	0.00017
13	2	12	-	12	3	10	373.10243	0.00022	19	1	19	-	19	0	19	394.69863	-0.00007
13	2	11	-	12	3	9	373.10243	0.00021	16	1	16	-	16	0	16	394.82751	0.00020
15	2	14	-	14	3	11	373.96822	0.00015	15	1	15	-	15	0	15	394.86617	0.00021
15	2	13	-	14	3	11	373.96822	0.00013	14	1	14	-	14	0	14	394.90222	0.00003
17	2	16	-	16	3	14	374.82552	-0.00006	11	1	11	-	11	0	11	394.99631	0.00010
17	2	15	-	16	3	13	374.82552	-0.00009	10	1	10	-	10	0	10	395.02316	0.00017
19	2	18	-	18	3	16	375.67491	0.00021	7	1	7	-	7	0	7	395.08831	0.00008
19	2	17	-	18	3	15	375.67491	0.00016									
23	2	22	-	22	3	20	377.34774	0.00008	6	1	5	-	5	0			

TABLE I—Continued

J	Ka	Kc	-	J	Ka	Kc	Observed	O-C	J	Ka	Kc	-	J	Ka	Kc	Observed	O-C
17	2	13	-	18	1	17	395.69817	-0.00008	14	3	11	-	13	2	11	419.80332	0.00006
16	2	15	-	17	1	17	396.25488	-0.00008	15	3	12	-	14	2	12	420.23435	0.00017
16	2	14	-	17	1	16	396.19888	-0.00003	17	3	13	-	16	2	15	421.08960	0.00013
15	2	13	-	16	1	15	396.69735	-0.00006	18	3	14	-	17	2	14	421.08960	0.00003
14	2	13	-	15	1	15	397.23757	-0.00012	18	3	16	-	17	2	15	421.31401	0.00013
11	2	9	-	12	1	11	398.66946	-0.00006	18	3	15	-	17	2	16	421.31401	0.00002
10	2	9	-	11	1	11	399.18105	-0.00018	20	3	18	-	19	2	18	421.31401	0.00016
9	2	7	-	10	1	9	399.64218	-0.00019	20	3	17	-	19	2	17	422.35636	0.00000
7	2	6	-	8	1	8	400.61939	-0.00017	21	3	19	-	20	2	19	422.77423	0.00014
6	2	5	-	7	1	7	401.09307	-0.00022	21	3	18	-	20	2	18	422.77423	-0.00006
23	2	23	-	25	1	23	403.75849	-0.00016	22	3	19	-	21	2	19	423.19007	0.00004
23	2	21	-	23	1	23	403.85111	-0.00007	23	3	21	-	22	2	21	423.60337	0.00005
22	2	20	-	22	1	22	403.89437	-0.00005	24	3	21	-	23	2	21	424.01508	0.00010
21	2	19	-	21	1	21	403.93604	-0.00015	25	3	23	-	24	2	23	424.42399	0.00020
19	2	17	-	19	1	19	404.01349	-0.00017	25	3	22	-	24	2	22	424.42399	-0.00019
16	2	17	-	18	1	17	403.86682	-0.00011	25	4	*	-	26	3	*	409.98739	-0.00007
17	2	15	-	17	1	17	404.08341	-0.00019	24	4	*	-	25	3	*	410.48167	-0.00001
13	2	14	-	15	1	14	404.10205	0.00001	23	4	*	-	24	3	*	410.99379	-0.00011
13	2	12	-	13	1	12	404.16736	-0.00015	20	4	*	-	21	3	*	412.31661	0.00013
12	2	11	-	12	1	11	404.19678	-0.00008	19	4	*	-	20	3	*	413.02270	0.00006
3	2	1	-	2	1	1	405.74828	-0.00012	17	4	*	-	18	3	*	414.02474	-0.00011
4	2	3	-	3	1	3	406.20430	-0.00019	16	4	*	-	17	3	*	414.52288	-0.00003
6	2	5	-	5	1	5	407.10860	-0.00018	15	4	*	-	16	3	*	415.01888	-0.00004
7	2	6	-	6	1	6	407.53787	-0.00018	14	4	*	-	15	3	*	415.51278	-0.00011
11	2	10	-	10	1	10	409.33580	-0.00006	12	4	*	-	13	3	*	416.49450	-0.00017
11	2	9	-	10	1	9	409.31560	-0.00011	10	4	*	-	11	3	*	417.46841	0.00020
12	2	11	-	11	1	11	409.77328	-0.00020	9	4	*	-	10	3	*	417.95182	-0.00007
13	2	11	-	12	1	11	410.18449	-0.00009	25	4	*	-	25	3	*	421.98630	0.00015
14	2	12	-	13	1	12	410.61537	-0.00018	24	4	*	-	24	3	*	422.03900	-0.00003
15	2	13	-	14	1	13	411.04408	-0.00013	23	4	*	-	23	3	*	422.08972	-0.00008
16	2	13	-	15	1	15	411.51430	-0.00020	22	4	*	-	22	3	*	422.13840	-0.00006
17	2	16	-	16	1	16	411.94429	-0.00009	21	4	*	-	21	3	*	422.18491	-0.00009
17	2	15	-	16	1	15	411.89448	-0.00008	20	4	*	-	20	3	*	422.23837	-0.00006
19	2	18	-	18	1	18	412.79818	-0.00008	19	4	*	-	19	3	*	422.27176	-0.00001
19	2	17	-	18	1	17	412.73580	0.00018	18	4	*	-	18	3	*	422.31192	-0.00003
20	2	18	-	19	1	18	413.15249	-0.00016	17	4	*	-	17	3	*	422.35010	0.00006
21	2	19	-	20	1	19	413.56728	-0.00006	16	4	*	-	16	3	*	422.38599	-0.00002
22	2	20	-	21	1	20	413.97979	0.00009	15	4	*	-	15	3	*	422.41971	-0.00016
23	2	21	-	22	1	21	414.38958	-0.00012	14	4	*	-	14	3	*	422.45163	0.00002
24	2	23	-	23	1	23	414.89831	-0.00015	13	4	*	-	13	3	*	422.48136	0.00012
24	2	22	-	23	1	22	414.79739	0.00002	12	4	*	-	12	3	*	422.50867	-0.00008
25	2	24	-	24	1	24	415.31240	-0.00017	11	4	*	-	11	3	*	422.53406	-0.00009
24	3	21	-	25	2	23	401.36042	0.00010	10	4	*	-	10	3	*	422.55734	-0.00005
23	3	21	-	24	2	23	401.87174	0.00013	9	4	*	-	9	3	*	422.57877	0.00017
22	3	19	-	23	2	21	402.38166	-0.00003	8	4	*	-	8	3	*	422.59737	-0.00008
21	3	19	-	22	2	21	402.88922	0.00010	6	4	*	-	6	3	*	422.62921	-0.00019
21	3	18	-	22	2	20	402.88922	-0.00018	4	4	*	-	3	3	*	424.50346	-0.00015
20	3	17	-	21	2	19	403.39321	0.00010	3	4	*	-	3	3	*	424.93573	0.00000
19	3	17	-	20	2	19	403.89869	0.00006	6	4	*	-	5	3	*	425.40571	0.00001
19	3	16	-	20	2	18	403.89869	-0.00013	7	4	*	-	6	3	*	425.85350	-0.00004
18	3	15	-	19	2	17	404.40064	0.00011	8	4	*	-	7	3	*	426.29918	-0.00005
17	3	15	-	18	2	17	404.90024	0.00013	9	4	*	-	8	3	*	426.74260	-0.00017
16	3	14	-	17	2	16	404.90024	0.00000	10	4	*	-	9	3	*	427.18410	-0.00005
16	3	13	-	17	2	15	405.39804	0.00011	11	4	*	-	10	3	*	427.62318	-0.00019
15	3	13	-	16	2	15	405.89372	0.00019	12	4	*	-	11	3	*	428.06053	0.00010
15	3	12	-	16	2	14	405.89372	0.00011	13	4	*	-	12	3	*	428.49328	-0.00004
14	3	12	-	15	2	14	406.38722	0.00002	14	4	*	-	13	3	*	428.92796	-0.00009
14	3	11	-	15	2	13	406.38722	-0.00004	13	4	*	-	12	3	*	429.35839	0.00000
13	3	10	-	14	2	12	406.87907	0.00018	16	4	*	-	15	3	*	429.78688	0.00000
12	3	10	-	13	2	12	407.36837	0.00012	18	4	*	-	17	3	*	430.63735	0.00020
12	3	9	-	13	2	11	407.36837	0.00009	20	4	*	-	19	3	*	431.47854	-0.00001
9	3	7	-	10	2	9	408.82518	0.00016	21	4	*	-	20	3	*	431.89584	-0.00012
9	3	6	-	10	2	8	408.82518	0.00015	22	4	*	-	21	3	*	432.31112	-0.00005
24	3	21	-	24	2	23	412.91814	0.00015	23	4	*	-	22	3	*	432.72414	-0.00002
22	3	19	-	22	2	21	413.01853	0.00011	24	4	*	-	23	3	*	433.13491	-0.00003
22	3	20	-	22	2	20	413.01853	-0.00018	25	4	*	-	24	3	*	433.54351	0.00000
21	3	19	-	21	2	19	413.06283	0.00010	25	5	*	-	26	4	*	419.04019	0.00014
20	3	17	-	20	2	19	413.10653	0.00003	24	5	*	-	25	4	*	419.53481	-0.00012
20	3	18	-	20	2	18	413.10653	-0.00014	23	5	*	-	24	4	*	420.06781	0.00004
19	3	16	-	19	2	18	413.14855	0.00019	22	5	*	-	23	4	*	420.57892	0.00004
19	3	17	-	19	2	17	413.14855	0.00003	21	5	*	-	22	4	*	421.08741	0.00006
18	3	15	-	18	2	17	413.18826	0.00011	18	5	*	-	19	4	*	422.60141	0.00006
18	3	16	-	18	2	16	413.18826	-0.00002	17	5	*	-	18	4	*	423.10190	0.00000
17	3	15	-	17	2	15	413.22607	0.00012	16	5	*	-	17	4	*	423.60031	-0.00008
16	3	13	-	16	2	15	413.26156	0.00011	15	5	*	-	16	4	*	424.09	





TABLE I—Continued

J	Ka	Kc	-	J	Ka	Kc	Observed	O-C	J	Ka	Kc	-	J	Ka	Kc	Observed	O-C	
14	4	*	-	15	5	*	341.32768	-0.00016	13	0	13	-	12	1	11	364.72342	0.00007	
13	4	*	-	14	5	*	341.81828	-0.00005	14	0	14	-	13	1	12	365.14991	0.00010	
12	4	*	-	13	5	*	342.30687	-0.00016	15	0	15	-	14	1	13	365.57401	0.00027	
11	4	*	-	12	5	*	342.79338	-0.00003	17	0	17	-	16	1	15	366.41391	-0.00011	
10	4	*	-	11	5	*	343.27807	0.00009	18	0	18	-	17	1	16	366.83060	0.00024	
9	4	*	-	10	5	*	343.76068	0.00008	21	0	21	-	20	1	19	368.06421	0.00020	
8	4	*	-	9	5	*	344.24118	-0.00006	22	0	22	-	21	1	20	368.46991	-0.00019	
7	4	*	-	8	5	*	344.71987	-0.00003	23	0	23	-	22	1	21	368.87581	0.00022	
6	4	*	-	7	5	*	345.19677	0.00019	25	0	25	-	24	1	23	369.67501	0.00021	
5	4	*	-	6	5	*	345.67138	0.00012										
4	4	*	-	5	5	*	346.14407	0.00012										
									e $\nu_2$ -3-2 Band - Low Freq. Comp.									
25	4	*	-	25	5	*	347.82090	0.00020	25	1	25	-	25	0	25	368.92621	0.00004	
24	4	*	-	24	5	*	347.87110	-0.00009	24	1	24	-	24	0	24	368.99363	-0.00013	
23	4	*	-	23	5	*	347.91959	-0.00007	19	1	19	-	19	0	19	367.29111	-0.00008	
22	4	*	-	22	5	*	347.96619	0.00008	18	1	18	-	18	0	18	367.34290	0.00033	
21	4	*	-	21	5	*	348.01047	-0.00008	17	1	17	-	17	0	17	367.39121	-0.00004	
19	4	*	-	19	5	*	348.05308	0.00011	15	1	15	-	15	0	15	367.46023	-0.00028	
18	4	*	-	18	5	*	348.09339	0.00001	13	1	13	-	13	0	13	367.55872	-0.00022	
17	4	*	-	17	5	*	348.13178	0.00002	11	1	11	-	11	0	11	367.62650	-0.00007	
16	4	*	-	16	5	*	348.16810	-0.00003	10	1	10	-	10	0	10	367.69610	-0.00022	
15	4	*	-	15	5	*	348.20249	0.00002	9	1	9	-	9	0	9	367.68320	-0.00017	
13	4	*	-	13	5	*	348.23478	-0.00002	7	1	7	-	7	0	7	367.72922	-0.00014	
12	4	*	-	12	5	*	348.26337	-0.00003	6	1	6	-	6	0	6	367.74842	0.00012	
11	4	*	-	11	5	*	348.31980	0.00013	4	1	4	-	4	0	4	367.77820	0.00013	
10	4	*	-	10	5	*	348.34400	0.00008	3	1	3	-	3	0	3	367.78913	0.00023	
9	4	*	-	9	5	*	348.36619	0.00004	2	1	2	-	2	0	2	367.79700	0.00001	
8	4	*	-	8	5	*	348.38639	0.00003										
							348.40439	-0.00016	6	1	6	-	6	0	6	370.53712	-0.00020	
20	4	*	-	19	5	*	357.30000	-0.00017	7	1	7	-	7	0	7	370.98723	-0.00004	
22	4	*	-	21	5	*	358.13658	-0.00012	8	1	8	-	8	0	8	371.43553	-0.00013	
23	4	*	-	22	5	*	358.55180	0.00000	10	1	10	-	10	0	10	372.32744	-0.00030	
24	4	*	-	23	5	*	358.96480	0.00001	15	1	15	-	15	0	15	374.53023	-0.00015	
25	4	*	-	24	5	*	359.37570	0.00004	16	1	16	-	16	0	16	374.96593	-0.00021	
									18	1	18	-	18	0	18	375.82393	0.00006	
									19	1	19	-	19	0	19	376.26393	0.00010	
									20	1	20	-	20	0	20	376.69322	0.00005	
									22	1	22	-	22	0	22	377.54693	-0.00010	
									24	1	24	-	24	0	24	378.39434	-0.00004	
									d $\nu_2$ -3-2 Band - High Freq. Comp.									
25	1	25	-	25	0	25	367.30091	-0.00004	24	2	23	-	24	1	23	376.23741	0.00006	
24	1	24	-	24	0	24	367.36753	-0.00011	23	2	21	-	23	1	23	376.49403	0.00002	
23	1	23	-	23	0	23	367.43152	-0.00014	20	2	18	-	20	1	20	376.61021	0.00001	
22	1	22	-	22	0	22	367.49311	0.00009	20	2	19	-	20	1	19	376.46052	-0.00004	
21	1	21	-	21	0	21	367.55161	-0.00010	19	2	17	-	19	1	19	376.64543	-0.00002	
19	1	19	-	19	0	19	367.66102	-0.00008	17	2	15	-	17	1	17	376.71075	0.00001	
17	1	17	-	17	0	17	367.75971	-0.00012	16	2	15	-	16	1	15	376.64422	0.00010	
15	1	15	-	15	0	15	367.84781	-0.00007	15	2	13	-	15	1	15	376.76933	0.00032	
14	1	14	-	14	0	14	367.88791	0.00000	14	2	12	-	14	1	14	376.79543	-0.00011	
13	1	13	-	13	0	13	367.92521	-0.00006	14	2	13	-	14	1	13	376.72084	-0.00016	
11	1	11	-	11	0	11	367.99201	0.00002	15	2	11	-	15	1	13	376.82002	-0.00026	
9	1	9	-	9	0	9	368.04801	-0.00002	12	2	11	-	12	1	11	376.78784	-0.00014	
7	1	7	-	7	0	7	368.09333	-0.00008	11	2	9	-	11	1	11	376.86465	0.00013	
5	1	5	-	5	0	5	368.12803	-0.00007	10	2	8	-	10	1	10	376.88423	0.00024	
									10	2	9	-	10	1	9	376.84524	0.00021	
17	1	16	-	16	0	16	375.76411	0.00001	25	0	25	-	25	1	25	358.00699	0.00004	
18	1	17	-	17	0	17	376.19664	-0.00011	24	0	24	-	24	1	24	358.05278	-0.00003	
20	1	19	-	19	0	19	377.03725	-0.00001	23	0	23	-	23	1	23	358.09520	-0.00007	
21	1	20	-	20	0	20	377.48483	-0.00027	21	0	21	-	21	1	21	358.17470	-0.00008	
22	1	21	-	21	0	21	377.91125	-0.00008	19	0	19	-	19	1	19	358.24721	0.00010	
24	1	23	-	23	0	23	378.75884	-0.00008	18	0	18	-	18	1	18	358.28039	0.00000	
25	2	23	-	25	1	25	376.78581	0.00008	17	0	17	-	17	1	17	358.31230	0.00001	
24	2	23	-	24	1	23	376.81444	-0.00011	16	0	16	-	16	1	16	358.34221	0.00000	
23	2	21	-	23	1	23	376.87115	0.00014	15	0	15	-	15	1	15	358.37028	-0.00007	
22	2	21	-	22	1	21	376.92024	0.00009	12	0	12	-	12	1	12	358.42158	0.00026	
21	2	19	-	21	1	21	376.94911	-0.00027	11	0	11	-	11	1	11	358.44458	0.00023	
20	2	19	-	20	1	19	376.85615	0.00019	9	0	9	-	9	1	9	358.46329	0.00007	
19	2	17	-	19	1	19	377.02102	0.00014	7	0	7	-	7	1	7	358.50209	0.00003	
17	2	15	-	17	1	17	377.08553	0.00009										
16	2	15	-	16	1	15	377.01824	0.00016										
15	2	13	-	15	1	15	377.14285	-0.00022										
14	2	12	-	14	1	14	377.16912	-0.00016	9	0	9	-	8	1	7	362.61941	-0.00011	
12	2	11	-	12	1	11	377.16104	0.00017	11	0	11	-	10	1	9	363.46971	0.00016	
10	2	9	-	10	1	9	377.21752	0.00001	13	0	13	-	12	1	11	364.34960	0.00010	
									18	0	18	-	17	1	16	366.45481	-0.00005	
									19	0	19	-	18	1	17	366.86611	-0.00012	
									20	0	20	-	19	1	18	367.27942	0.00041	
									21	0	21	-	20	1	19	367.68741	0.00021	
									23	0	23	-	22	1	21	368.49561	-0.00014	

RECEIVED: March 27, 1989

## REFERENCES

1. G. WINNEWISSER, M. WINNEWISSER, AND W. GORDY, *J. Chem. Phys.* 49, 3465-3478 (1968).
2. G. WINNEWISSER, *J. Chem. Phys.* 56, 2944-2954 (1972); *J. Chem. Phys.* 57, 1803-1804 (1972); *J. Mol. Spectrosc.* 41, 534-547 (1972).
3. G. WINNEWISSER AND P. HELMINGER, *J. Chem. Phys.* 56, 2955-2966 (1972); *J. Chem. Phys.* 56, 2967-2979 (1972).
4. F. FEHER AND M. BAUDLER, *Z. Elektrochem.* 47, 844-848 (1941).
5. M. K. WILSON AND R. M. BADGER, *J. Chem. Phys.* 17, 1232-1236 (1949).
6. R. L. REDINGTON, *J. Mol. Spectrosc.* 9, 469-476 (1962).

7. B. P. WINNEWISSER AND M. WINNEWISSER, *Z. Naturforsch. A* 23, 832-839 (1968).
8. M. WINNEWISSER AND J. HAASE, *Z. Naturforsch. A* 23, 56-60 (1968).
9. B. P. WINNEWISSER, *J. Mol. Spectrosc.* 36, 414-432 (1970).
10. G. M. PLUMMER, G. WINNEWISSER, M. WINNEWISSER, J. HAHN, AND K. REINARTZ, *J. Mol. Spectrosc.* 126, 255-269 (1987).
11. E. HERBST AND G. WINNEWISSER, *Chem. Phys. Lett.* 155, 572-575 (1989).
12. K. JOLMA, V.-M. HORNERMAN, J. KAUPPINEN, AND A. G. MAKI, *J. Mol. Spectrosc.* 113, 167-174 (1985).
13. G. SCHWAHN, R. SCHIEDER, M. BESTER, AND G. WINNEWISSER, *J. Mol. Spectrosc.* 116, 263-270 (1986).
14. R. H. HUNT, R. A. LEACOCK, C. W. PETERS, AND K. T. HECHT, *J. Chem. Phys.* 42, 1931-1946 (1965).
15. H. DREIZLER, *Z. Naturforsch. A* 21, 1628-1632 (1966).
16. J. T. HOUGEN, *Canad. J. Phys.* 62, 1392-1402 (1984).
17. W. GORDY AND R. L. COOK, "Microwave Molecular Spectra," A. Weissberger, Ed., *Techniques of Chemistry*, Vol. 18, Wiley, New York, 1984.
18. P. R. BUNKER, "Molecular Symmetry and Spectroscopy," Academic Press, New York, 1979.
19. F. GREIN, *Chem. Phys. Lett.* 116, 323-325 (1985).
20. D. A. DIXON, D. ZEROKA, J. J. WENDOLOSKI, AND Z. R. WASSERMAN, *J. Phys. Chem.* 89, 5334-5336 (1985).
21. E. HERBST, J. K. MESSER, F. C. DE LUCIA, AND P. HELMINGER, *J. Mol. Spectrosc.* 108, 42-57 (1984).
22. W. C. BOWMAN, P. HELMINGER, AND F. C. DE LUCIA, *J. Mol. Spectrosc.* 87, 571-574 (1981). See also P. HELMINGER, W. C. BOWMAN, AND F. C. DE LUCIA, *J. Mol. Spectrosc.* 85, 120-130 (1981).
23. E. HERBST, G. WINNEWISSER, K. M. T. YAMADA, AND D. J. DEFREES, submitted to *J. Chem. Phys.*